



Munich Personal RePEc Archive

Hexagonal distributions of cities in Southern Germany and Eastern USA: Group-theoretic spectrum analysis

Ikeda, Kiyohiro and Murota, Kazuo and Takayama, Yuki
and Kamei, Motohiro

Department of Civil and Environmental Engineering, Tohoku
University, School of Business Administration, Tokyo Metropolitan
University, Kanazawa University, East Nippon Expressway
Company Limited

12 May 2017

Online at <https://mpra.ub.uni-muenchen.de/79085/>
MPRA Paper No. 79085, posted 12 May 2017 16:40 UTC

Hexagonal distributions of cities in Southern Germany and Eastern USA: Group-theoretic spectrum analysis

Kiyohiro Ikeda,¹ Kazuo Murota,² Yuki Takayama,³ Motohiro Kamei⁴

Abstract

Cities in Southern Germany are envisaged to form hexagonal distributions in central place theory; however, rigorous verification of this theory has been lacking over years. To support this theory, we introduce a group-theoretic Fourier spectrum analysis that can detect geometrical patterns of cities based on the statistical population data. In addition to hexagonal patterns in the theory, we propose a core–satellite pattern. Using this analysis, we detected a strong power spectrum for this pattern for population data in Southern Germany. Moreover, a gigantic hexagonal distribution of cities in Eastern USA was found to be an assemblage of the core–satellite and hexagonal patterns. The amazing geometrical regularity of this distribution implies the existence of such patterns in the real world, thereby underpinning the theory.

¹Address for correspondence: Kiyohiro Ikeda, Department of Civil and Environmental Engineering, Tohoku University, Aoba, Sendai 980-8579, Japan; kiyohiro.ikeda.b4@tohoku.ac.jp

²School of Business Administration, Tokyo Metropolitan University, Tokyo 192-0397, Japan

³Institute of Science and Eng., Kanazawa University, Kakuma, Kanazawa 920-1192, Japan

⁴East Nippon Expressway Company Limited, Mihama, Chiba 261-0014 Japan

Keywords: central place theory; city distribution; hexagonal pattern; spectrum
analysis, statistical analysis

1. Introduction

Cities are cradles of economic development and are prospering worldwide with a tendency for more and more people to live there. Extensive studies of cities have been conducted from various points of view as explained in the related studies surveyed in Section 2.

In central place theory in economic geography, self-organization of a hexagonal distribution in a hierarchy of urbanization (megalopolises, cities, towns, villages, etc.) was envisaged based on a study of Southern Germany by Christaller (1933) [10] (Fig. 1(a)) and a distribution comprising overlapping hexagons of different sizes was proposed by Lösch (1940) [35] (Fig. 1(b)). Christaller posed questions: “But how can we find a general explanation for the sizes, number, and distribution of towns? How can we discover the laws?” A partial answer to these questions was given by the studies of the size distribution of cities (Section 2). The geographical distribution of cities is a question which remains to be resolved and is a focus of this paper as elucidation of its mechanism would be vital for the successful future design of urban infrastructures.

Although there has been a mixed response to central place theory,⁵ its reemer-

⁵Fujita, Krugman, and Mori (1999, p.212) [20] stated “it [central place theory] is a powerful idea too good for being left as an obscure theory.”

gence in regional science has come to be acknowledged (Mulligan, Partridge, and Carruthers, 2012 [38]). In this theory, the existence of hexagonal agglomerations in the real world was shown only schematically. A rigorous verification of the existence in the real world has been lacking over years, notwithstanding extensive attempts at such verification (Section 2). It is not too much to say that such a lack may be impeding the systematic application of this theory to the real data.

That said, this paper aims to search for hexagonal agglomerations in the real world in a more systematic and scientific manner. For this purpose, we refer to a standpoint of pattern formation: self-organization of hexagonal patterns from uniformity was observed in various physical phenomena (see, e.g., Golubitsky and Stewart, 2002 [22]), just as hexagonal distributions of central places are envisaged to be self-organized (Christaller, 1933 [10]).

The major target of this paper is to propose an analysis procedure to detect hexagonal patterns. Spectrum analysis is a standard tool to detect the occurrence of pattern formation. Instead of a naïve double Fourier series in rectangular coordinates, for which the connection to hexagonal patterns would not be clear, this paper proposes a group-theoretic spectrum analysis procedure based on the theory on self-organizing hexagons on a hexagonal lattice (Ikeda and Murota, 2014 [26]).

An oblique Fourier series on a finite hexagonal lattice is regrouped into an

ensemble of components, which are related to self-organizing hexagonal patterns of various kinds.⁶ The present spectrum analysis proceeds as follows: (i) A data of population distribution of an ensemble of cities on a rhombic domain is discretized to the nodes on a hexagonal lattice covering this domain. (ii) A predominant spectrum of this data is found and the associated spatial pattern is set forth as an underlying spatial pattern of cities.

The proposed analysis procedure was applied to the population data of Southern Germany and Eastern USA. This paper poses a question: “Do spatially repeated hexagonal distributions exist in Southern Germany?” To answer this question, the population data of Southern Germany in 2011 was processed by the present Fourier series. As a consequence, we found a hexagonal network of cities surrounding Stuttgart, thereby scientifically underpinning that theory.

The search of hexagonal patterns was extended to Eastern USA, in which a large number of cities are spread over a large expanse of flat area. The city lights of the USA (Fig. 2) display apparent geometrical patterns that have motivated this search of their underlying mechanism. By the present spectrum analysis, a gigantic hexagonal distribution of cities in Eastern USA was found for the population

⁶The connection between the oblique Fourier series and self-organizing hexagonal patterns was studied in bifurcation theory (e.g., Golubitsky, Stewart, and Schaeffer, 1988 [23]; Ikeda and Murota, 2014 [26]).

data in 2014. The amazing geometrical regularity of this distribution implies the existence of hexagonal patterns in the real world.

This paper is organized as follows. Related studies are presented in Section 2. A group-theoretic double Fourier series on a hexagonal lattice is advanced in Section 3. Hexagonal distributions of cities are detected in the population data of Southern Germany in Section 4 and of Eastern USA in Section 5.

2. Related studies

Spatial evolution of cities is an important topic in regional science and has been studied theoretically and statistically based on population data of various countries. Whereas there are a large number of works on this topic, we introduce those related to Germany and the USA, which are the targets of this paper. German division and reunification were studied by Redding and Sturm (2008) [43]. The city size distribution of West Germany was investigated by Bosker et al. (2008) [7] and Findeisena and Südekum (2008) [18]. Evolution of cities in the USA has been studied from various viewpoints: city size distribution (Overman and Ioannides, 2001; Black and Henderson, 2003 [6]; González-Val, 2010 [24]), spatial features (Ioannides and Overman, 2004 [30]), migration (Davies, Greenwood, and Li, 2001 [12]), density of urban areas (Kim 2007 [31]), and urban hierarchy distance (Partridge et al., 2008 [42]).

Bridging empirics and theory (e.g., New Economic Geography) is regarded as an important topic (e.g., Stelder, 2005 [46]; Bosker et al., 2010 [8]), and the reemergence of central place theory with its complements, such as NEG models, has come to be acknowledged (Mulligan, Partridge, and Carruthers, 2012 [38]).

Several attempts to simulate the self-organization of central place systems have been conducted through modeling of economic mechanisms of agglomerations.⁷ A dynamic model based on central place theory was used to successfully calibrate a model with socio-economic data for Belgium, 1970–84 (Sanglier and Allen, 1989 [45]). Mori and Smith (2011) [37] developed an industrial agglomeration approach to central place and city size regularities. Zipf’s law is extensively used to explain size distribution.⁸

There are studies of cities focusing on their various aspects. The geometry of cities was explained by fractal (Batty and Longley, 1994 [3]). The distributions of satellite cities, towns, and villages around Berlin and London were shown to follow a universal law (Makse et al., 1995 [36]). Sociodynamics was used to express migration by Munz and Weidlich (1990) [39] and Weidlich (2000) [48].

⁷See, e.g., Eaton and Lipsey (1975, 1982) [15, 17], Clarke and Wilson (1983) [11], Krugman (1993) [33], Weidlich and Haag (1987) [49], Munz and Weidlich (1990) [39], and Fujita, Krugman, and Mori (1999) [20].

⁸See, e.g., Gabaix (1999) [21], Duranton (2006) [14], and Rossi-Hansenberg and Wright (2007) [44]. See also Hsu, Mori, and Smith (2014) [25] and references therein.

Scaling of cities was studied by Batty (2008, 2013) [1, 2] and Bettencourt (2013) [4]. The formation of a city was investigated using the percolation theory and GIS data of 29 cities (Bitner et al., 2009 [5]).

Hexagonal distributions were inferred to be self-organized in two dimensions by Krugman (1996, p.91) [34]. Indeed, hexagonal patterns on a hexagonal lattice were shown to exist theoretically and were simulated (Ikeda et al., 2012, 2014 [27, 28]; Ikeda and Murota, 2014 [26]) using a model by Forslid and Ottaviano (2003) [19]. Bifurcating hexagonal distributions were studied in nonlinear mathematics (e.g., Golubitsky, Stewart, and Schaeffer, 1988 [23]). There are several studies of spatial agglomeration on a square lattice.⁹

3. Group-theoretic spectrum analysis

A group-theoretic spectrum analysis procedure is introduced as a systematic tool to detect hexagonal agglomerations in the real world. An oblique Fourier series on a finite hexagonal lattice is regrouped into an ensemble of components, which are related to hexagonal patterns of various kinds. The procedure is used to detect hexagonal distributions in the statistical data of population in Sections 4 and 5.

⁹See, e.g., Clarke and Wilson (1983) [11], Weidlich and Haag (1987) [49], Munz and Weidlich (1990) [39], Brakman et al. (1999) [9], and Stelder (2005) [46].

3.1. Hexagonal lattice and Lösch's hexagons

As spatial platforms of hexagonal distributions, an infinite hexagonal lattice and a finite one are employed. The infinite one is a two-dimensional discretized uniform space that expresses a boundless isotropic plain in central place theory (Dicken and Lloyd, 1990 [13]). The finite one with periodic boundary conditions is advanced as a spatial platform for the investigation of agglomeration patterns in the real world (Ikeda and Murota, 2014 [26]).

An infinite hexagonal lattice (Fig. 3(a)) is given as a set of integer combinations of oblique basis vectors $\boldsymbol{\ell}_1 = d(1, 0)^\top$ and $\boldsymbol{\ell}_2 = d(-1/2, \sqrt{3}/2)^\top$, where $d > 0$ means the length of these vectors. Lösch's hexagonal distribution on the lattice is represented by a sublattice spanned by

$$\boldsymbol{t}_1 = \alpha\boldsymbol{\ell}_1 + \beta\boldsymbol{\ell}_2, \quad \boldsymbol{t}_2 = -\beta\boldsymbol{\ell}_1 + (\alpha - \beta)\boldsymbol{\ell}_2, \quad (1)$$

where α and β are integer-valued parameters with $(\alpha, \beta) \neq (0, 0)$. Figure 3(b) denotes a hexagon on a sublattice for $(\alpha, \beta) = (2, 1)$. The *normalized spatial period* L/d of the sublattice is defined using the (common) length of the basis vectors \boldsymbol{t}_1 and \boldsymbol{t}_2 , and is given by $L/d = \sqrt{D}$ with $D = \alpha^2 - \alpha\beta + \beta^2$ characterizes the size of the hexagon.

A finite hexagonal lattice comprises a system of uniformly distributed $n \times n$ places; see, for example, Fig. 4(a) for the 3×3 hexagonal lattice. Discretized

degrees-of-freedom are allocated to each node of the lattice. Periodic boundary conditions are used to express uniformity and to avoid heterogeneity due to the boundaries (Fig. 4(b)). The finite lattice with size $n = 18$, which is employed in this paper (Appendix A), can encompass Lösch's hexagons with the following sizes $D = 1, 3, 4, 9, 12, 27, 36, 81, 108, 324$.

3.2. Outline of group-theoretic bifurcation theory

In a spatial agglomeration model on the hexagonal lattice, we consider an equilibrium condition

$$\mathbf{F}(\boldsymbol{\lambda}, \tau) = \mathbf{0}, \quad (2)$$

where $\boldsymbol{\lambda}$ is a scalar field defined on the nodes of the lattice and τ is a parameter.¹⁰

This equilibrium condition is quite general and is applicable to any problems with a scalar field defined on the nodes of the lattice.

We can derive a transformation matrix Q that puts the Jacobian matrix $J = \partial \mathbf{F} / \partial \boldsymbol{\lambda}$ into a block-diagonal form:

$$Q^T J Q = \begin{bmatrix} \ddots & & O \\ & J^{(m)} & \\ O & & \ddots \end{bmatrix}. \quad (3)$$

¹⁰In a study for the 6×6 hexagonal lattice (Ikeda, Murota, and Takayama, 2017, [29]), λ was chosen as populations of mobile workers, τ as the transport cost parameter, and the equilibrium condition \mathbf{F} was defined using the replicator dynamics in the Forslid and Ottaviano model (2003) [19].

Here (m) labels each block and Q is made up of block matrices Q^u as

$$Q = [\dots, Q^{(m)}, \dots], \quad J^{(m)} = (Q^{(m)})^\top J Q^{(m)}. \quad (4)$$

Furthermore, we have $Q^{(m)} = (\mathbf{q}_i^{(m)} \mid i = 1, \dots, M(m))$ and each block consists of the basis vectors $\mathbf{q}_i^{(m)}$, which are given by discrete cosine and sine series (Appendix A). The matrix Q is dependent only on the lattice size and is independent on the economic modeling of the equilibrium condition (2).

Bifurcating patterns from the uniform state are self-organized when some block $J^{(m)}$ becomes singular. Each m labels a hexagon of a different kind.

3.3. Group-theoretic Fourier series and self-organizing hexagons

There are the patterns with hexagonal symmetry of 37 kinds associated with a set L_{hexa} of the labels m of diagonal blocks defined by

$$L_{\text{hexa}} = \{1, 3, 4, 9, 12, 27(\text{I}), 27(\text{II}), 27(\text{III}), 36(\text{I}), 36(\text{II}), \\ 81(\text{I}), \dots, 81(\text{VI}), 108(\text{I}), \dots, 108(\text{VI}), 324(\text{I}), \dots, 324(\text{XV})\}. \quad (5)$$

Here these labels imply the size D of hexagons (Table 1); for example, 27(I), 27(II), and 27(III) represent three different patterns with the same size $D = 27$.

Of the possible bifurcating patterns from a uniform state on this lattice, we focused on the 37 patterns with hexagonal symmetry that are given as¹¹ (Ikeda

¹¹In comparison with the previous study for the 6×6 hexagonal lattice (Ikeda, Murota, and

and Murota, 2014 [26]):

$$\mathbf{q}_{\text{hexa}}^{(m)} = \begin{cases} \mathbf{q}^{(3)} & \text{for } m = 3 \text{ with } M(m) = 2, \\ \mathbf{q}_1^{(4)} + \mathbf{q}_2^{(4)} + \mathbf{q}_3^{(4)} & \text{for } m = 4 \text{ with } M(m) = 3, \\ \mathbf{q}_1^{(m)} + \mathbf{q}_3^{(m)} + \mathbf{q}_5^{(m)} & \text{for } m\text{'s with } M(m) = 6, \\ \sum_{i=1}^6 \mathbf{q}_{2i-1}^{(m)} & \text{for } m\text{'s with } M(m) = 12. \end{cases} \quad (6)$$

See Figs. 5 and A2 for these patterns, which contain hexagons in central place theory, but also other patterns, which are beyond the scope of this theory.

The hexagons $\mathbf{q}_{\text{hexa}}^{(m)}$ with $m = 324(\text{I})$, $108(\text{I})$, $81(\text{I})$, and $36(\text{I})$, which are respectively called $\mathbf{q}^{\text{Megalopolis}}$, \mathbf{q}^3 hexagons, \mathbf{q}^4 hexagons, and \mathbf{q}^9 hexagons herein (Fig. 5(a)),¹² play a vital role in the search for distributions of cities in Sections 4 and 5. These patterns represent hexagons with a one-level hierarchy as identical blue circular zones expressing agglomeration are repeated to form a regular-hexagonal array.

In addition to these hexagons in central place theory, we focus on a “core-satellite pattern” for $m = 324(\text{IV})$, which is termed $\mathbf{q}^{\text{Core-satellite}}$. This pattern represents a large circle at the center surrounded by six small ellipses (Fig. 5(b)),¹³ and

Takayama, 2017, [29]), more diverse and realistic patterns have been found for the 18×18 hexagonal lattice in this paper.

¹²For an economic geography model on a hexagonal lattice, equilibria associated with \mathbf{q}^9 hexagons, \mathbf{q}^4 hexagons, \mathbf{q}^3 hexagons, and $\mathbf{q}^{\text{Megalopolis}}$ were shown to exist and to become stable in this order as the transport cost decreases from a large value (Ikeda, Murota, and Takayama, Fig.10, 2017 [29]).

¹³The rhombic domain of the pattern is made up of six large and two small regular triangles and

is interpreted as a two-level hierarchy with a circular downtown area (A-center) surrounded by six satellite places (B-centers). There are spatially shifted variants of this pattern (Fig. 5(d)). Although the pattern is not given much attention up to now,¹⁴ it plays a pivotal role in the description of the distribution of cities.

There are other bifurcating patterns (Fig. 5(e)). Spatial regularity is absent in non-bifurcating ones (Fig. 5(f)).

Although the 18×18 hexagonal lattice contains as many as 324 possible spectra, the number of spectra employed for discussion can be reduced based on the following two steps: (i) The 324 possible spectra can be decomposed into 37 subsets associated with the diagonal blocks in (3). (ii) Among the 37 bifurcating patterns for these blocks, we can focus on those which become dominant in a specific set of population data of a certain area.

3.4. Group-theoretic spectrum analysis

A group-theoretic double Fourier series in oblique coordinates along the finite hexagonal lattice is introduced. The population distribution λ can be expanded to

three rectangles, whereas the hexagonal patterns in central place theory are made up of a series of identical triangles. The pattern is robust against an increase in mesh size (see Fig. 5(c) for the pattern for the 24×24 hexagonal lattice).

¹⁴More attention was given to hexagons (Ikeda et al., 2012, 2014 [27, 28] and Ikeda and Murota, 2014 [26]) and a megalopolis pattern expressing centralization (Ikeda, Murota, and Takayama, 2017 [29]).

a group-theoretic double Fourier series as

$$\lambda = \sum_{m \in L_{\text{hexa}}} \sum_{i=1}^{M(m)} c_i^{(m)} \mathbf{q}_i^{(m)} \quad (7)$$

with Fourier coefficients $c_i^{(m)}$.

As a statistical tool to detect spatial patterns of distributions of cities, we introduce a group-theoretic spectrum analysis procedure. Compatibly with the hexagonal patterns of interest, we assemble the double Fourier components¹⁵ corresponding to a particular m in (7) as

$$\mathbf{q}^{(m)} = \sum_{i=1}^{M(m)} c_i^{(m)} \mathbf{q}_i^{(m)}. \quad (8)$$

The vector $\mathbf{q}^{(m)}$ for appropriately chosen $c_i^{(m)}$ can be associated with a hexagon that bifurcates from a uniform state, its size being implied by m . Then the double Fourier series in (7) is rewritten as

$$\lambda = \sum_{m \in L_{\text{hexa}}} \mathbf{q}^{(m)}. \quad (9)$$

A group-theoretic spectrum analysis procedure proposed herein proceeds as follows: (i) Observe the squared magnitudes $\|\mathbf{q}^{(m)}\|^2$ ($m \in L_{\text{hexa}}$) of these vectors ($\|\cdot\|$ is the Euclidean norm). (ii) Detect the wave numbers m of the predominant spectra (except for that of the uniform population $\mathbf{q}^{(1)}$). (iii) Inspect the associated

¹⁵These are so-called *isotypic components* in group-theoretic bifurcation theory (e.g., Golubitsky, Stewart, and Schaeffer, 1988 [23] and Ikeda and Murota, 2014 [26]).

spatial patterns $q^{(m)}$ to set forth an underlying spatial pattern of cities. More details of this procedure are given in Sections 4 and 5 based on actual data.

4. Hexagonal distribution of cities in Southern Germany

Hexagonal distributions of cities and towns of various sizes in Southern Germany were envisaged by Christaller (1933) [10]. Yet the existence of such distributions in the real world remains to be verified in a more rigorous manner. We would like to find a hexagonal pattern in the population data of Southern Germany in 2011 by the group-theoretic spectrum analysis (Section 3). Christaller's distribution of Stuttgart surrounded by five cities, München, Frankfurt, Nürnberg, Strasbourg, and Zürich (Fig. 6(a)) is the target of the present analysis. It is to be noted in advance that this distribution is not hexagonal but pentagonal and the distance between München and Zürich looks too long in comparison with other distances.

4.1. Population data and setting of the group-theoretic spectrum analysis

A rhombic domain in Southern Germany in 2011 was chosen based on a series of preliminary analyses (Fig. 6(b)). The domain was overlaid by an 18×18 regular-triangular mesh and the population was allocated to the nearest node to arrive at the discretized population distribution in Fig. 6(c).

The domain contains Southern Germany, as well as small parts of Austria, France, Netherlands, and Luxembourg. The population data were taken from the City Population website (<http://www.citypopulation.de/>), which is based on the original sources listed in Table 2. Based on population size, cities were classified into A-centers at Zürich and München; B-centers at Frankfurt and Stuttgart; C-centers at Nürnberg, Strasbourg, Mulhouse, and Saarbrücken; and D-centers at Konstanz and Basel (Table 3). The latitude and longitude of a location were acquired by GoogleMap and Nominatim of OpenStreetMap (<https://nominatim.openstreetmap.org/>).

4.2. Hexagonal satellite cities surrounding Stuttgart

Spectrum analysis of the discretized data on an 18×18 hexagonal lattice (Fig. 6(c)) was conducted to obtain the squared magnitudes $\|\mathbf{q}^{(m)}\|^2$ ($m \in L_{\text{hexa}}$) of the assembled Fourier terms in (9) (Fig. 6(d)).¹⁶ The core–satellite pattern $\mathbf{q}^{\text{Core–satellite}}$ had by far the largest magnitude among $\mathbf{q}^{(m)}$'s. The spatial pattern for $\mathbf{q}^{\text{Core–satellite}}$ ($= \mathbf{q}^{324(\text{IV})}$), which is depicted in Fig. 6(d), is in good agreement with the theoretical one in Fig. 5(b).

This pattern displays seven blue circular or elliptic zones of agglomeration

¹⁶In this figure and in the remainder of this paper, the squared magnitude $\|\mathbf{q}^{(1)}\|^2$ for the uniform distribution is suppressed since such a distribution is not of interest in the present study.

(Fig. 6(d)). These zones, which are depicted in the real population distribution (Fig. 6(c)), encompass most major cities in Southern Germany except for those along Rhine River. In view of this, it was straightforward to choose the four larger cities, München, Frankfurt, Stuttgart, and Nürnberg, which form a clear rhombic shape comprising two (regular) triangles. Strasbourg was chosen consistently with Christaller's distribution (Fig. 6(a)), while Saarbrücken could be a possible alternative. Yet we encountered a problem in that Zürich is located at the middle of two elliptic zones of agglomeration. As a remedy of this, Konstanz was included and a zone of Zürich–Mulhouse via Basel was chosen in place of Zürich to arrive at the hexagonal (core–satellite) pattern (Fig. 6(e)).

In this manner, we have arrived at a hexagonal distribution of Stuttgart surrounded by six cities, Frankfurt, München, Nürnberg, Strasbourg, Zürich–Mulhouse, and Konstanz (Fig. 6(e)) with an average inter-city distance of approximately 150 km. Thus, with the help of the present spectrum analysis, we have succeeded in depicting a hexagonal network of cities, instead of the pentagonal one by Christaller.

The distribution of the cities presented herein (Fig. 6(e)) looks like a $k = 3$ system based on the *market principle* (Christaller, 1933 [10]). Stuttgart (B-center) is surrounded by three regular-triangular-shaped first-level places of München (A-

center), Zürich (A-center), and Frankfurt (B-center).

The core–satellite pattern presented herein contains Christaller’s pentagonal distribution (Fig. 6(a)), thereby scientifically underpinning central place theory. That pattern is skewed towards Strasbourg, Zürich, and Konstanz due to the geographical borders of the Alps towards the south and Rhine River, Schwarzwald, and Vosges towards the west (Fig. 6(e)). Although Southern Germany is the origin of central place theory, it is not a boundless isotropic plain as assumed in this theory (Dicken and Lloyd, 1990 [13]). A clearer hexagonal pattern is to be found in a wider flat area in Eastern USA (Section 5).

4.3. Time evolution of spectra

A time evolution of the spectra of the population in the domain in Fig. 6(b) in the period from 1987, via 2000, to 2011 was studied. During this period, the population grew steadily and significantly from 32.6 million, via 36.1 million, to 37.0 million.

The evolution of the spectra for the increment of the population in the periods 1987–2000 and 2000–2011 was observed. In the period 1987–2000, an increase of the population was spread over the northeastern part of the domain (the left of Fig. 7(a)). There were strong spectra for the megalopolis pattern around the northeastern part of the domain (the right of Fig. 7(a)). This pattern of population

increment may be under the influence of the epoch-making event of the German reunification in 1990.

A phase shift was observed in the period 2000–2011; the core–satellite pattern was the strongest spectrum (Fig. 7(b)). This pattern indicates current and future trends of agglomeration to core places, such as München, Frankfurt, Stuttgart, Nürnberg, Strasbourg, and Zürich. These core places had been envisaged as central places in Southern Germany by Christaller (Fig. 6(a)).

Thus, we have arrived at a view of time evolution of agglomerating places. Whereas standard central place theory is static, the present spectrum analysis procedure presents a quasi-dynamic view based on time evolution of population, which is an important topic in regional science (Section 2).

The spectra in 1987 and those in 2000 are shown in Fig. 8. These spectra, as well as those in 2011 presented in Fig. 6(d), are quite similar (not optically discernible), thereby showing the robustness of these cross-sectional spectra against microeconomic changes in the period 1987–2011 although this period includes the German reunification in 1990.

5. Hexagonal network of cities in Eastern USA

After the successful search for the hexagonal city network in Southern Germany in Section 4, we proceed to deal with Eastern USA, in which a large number of cities are spread over a large expanse of flat area. A gigantic hexagonal city network there is constructed by assembling a series of hexagonal and core–satellite patterns. This is literally a challenge like a large jigsaw puzzle with many pieces.

5.1. Population data and outline of the spectrum analysis

The population data of Eastern USA in 2014 were taken from the City Population website (<http://www.citypopulation.de/>) based on the sources listed in Table 2. Based on population size, cities were classified from an A-center at New York, B-centers at Chicago, Dallas, Houston, Washington, and Atlanta, . . . to F-centers (Table B1 in Appendix B). Based on geography, Eastern USA was divided into Gulf Coast, South Atlantic, East and West North Central, and Middle Atlantic Regions. Similarly to the analysis of Southern Germany (Section 4), population of each rhombic domain for the spectrum analysis was discretized to the nodes of a 18×18 hexagonal lattice.

A series of preliminary group-theoretic spectrum analysis of the population data was conducted to detect the 18 rhombic domains belonging to five regions,

accommodating hexagonal and core–satellite patterns of cities (Fig. 9), as explained in the following subsection for individual regions. These domains were selected based on the two criteria: (i) the existence of a predominant spectrum and (ii) the compatibility of the spatial pattern for this spectrum with the real population distribution. The patterns found herein were assembled to set forth a gigantic hexagonal distribution (Fig. 10). There is a hierarchy of subnetworks with different geographical scales that look like the overlapping hexagons of Lösch (1940) [35].

The distribution encompasses many major cities there, except for some parts of the Atlantic seaboard, the Appalachian Mountains, and the Florida peninsula. The Mississippi River does not influence the patterns so much, while the distribution becomes sparser near the Appalachian Mountains, just as the hexagonal Bénard cell becomes less clear near the boundary (Koschmieder, 1993 [32]).

5.2. City subnetworks in individual regions in Eastern USA

Characteristic spatial patterns observed in city subnetworks in individual regions in Eastern USA are presented below.

Four large rhombic cities in Eastern USA: We begin with the largest Eastern USA Domain in Fig. 9(a). For the discretized population distribution of this domain on the 18×18 mesh in Fig. 11(a), the spectra of the squared magnitudes

$\|\mathbf{q}^{(m)}\|^2$ ($m \in L_{\text{hexa}}$) in Fig. 11(b) were computed, and, in turn, to find two competing strong spectra for $\mathbf{q}^{4 \text{ hexagons}}$ and $\mathbf{q}^{\text{Megalopolis}}$. The pattern $\mathbf{q}^{4 \text{ hexagons}}$ displays a 2×2 hexagons comprising rhombic-shaped four cities: New York, Chicago, Dallas, and Atlanta, whereas $\mathbf{q}^{\text{Megalopolis}}$ displays a megalopolis pattern at New York. These two patterns are superposed to arrive at $\mathbf{q}^{4 \text{ hexagons}} + \mathbf{q}^{\text{Megalopolis}}$ at the top of Fig. 11(b), which can be interpreted as a two-level hierarchy shown in (c), comprising an A-center at New York and three B-centers. In addition, we can observe an industrial belt between New York and Chicago, which is analyzed in detail later for the East North Central Region.

A 3×3 hexagonal array of cities in West North Central: West North Central Domain I centered on St. Louis (Fig. 9(a)) serves as the backbone of the city network in Eastern USA. For the discretized population distribution of this domain (Fig. 12(a)), the pattern $\mathbf{q}^{9 \text{ hexagons}}$ with nine rhombic hexagons had the strongest spectrum (Fig. 12(b)). This pattern can be interpreted as a 3×3 hexagonal array of cities in (c), encompassing: a B-center at Chicago, a C-center at Detroit, and D-centers at Cincinnati, St. Louis, Kansas City, and so on. These cities are located with an amazing geometrical regularity, the average distance between them being 435 km. This distance is more than twice that of Southern Germany, 150 km.

The clearest hexagonal distribution in Gulf Coast: In a wide expanse of flat area in the Gulf Coast Region, the four domains shown in Fig. 9(b) were extracted. The spectrum analysis was conducted on these domains to find that the core–satellite pattern $q^{\text{Core-satellite}}$ was predominant for all the domains (Fig. B1 in Appendix B). These patterns are interpreted as networks of cities depicted in Fig. 13(a). There are two core–satellite patterns centered on Birmingham and Jackson, respectively; in particular, the pattern centered on Birmingham has a regular shape (yellow lines in Fig. 13(b)). These patterns are sandwiched by a pair of shifted core–satellite patterns. The patterns in these four domains are found to be compatible with each other and, in turn, to be assembled into a hexagonal network of cities with a geometrical regularity from Dallas to Atlanta along the Gulf of Mexico (Fig. 13(b)). This network merges compatibly with the south border of the 3×3 hexagonal distribution centered on St. Louis. Thus, this wide expanse of flat area accommodates a hexagonal pattern, just as hexagonal patterns in physics emerge from uniformity (Koschmieder, 1993 [32]).

Fine hexagonal distributions in three directions in South Atlantic: By the spectrum analysis of the South Atlantic Region (see Fig. B2 for the population distributions and the spectra), three core–satellite patterns and two shifted ones were found (Fig. 14(a)). These patterns are geometrically compatible with each

other and can be assembled into hexagonal distributions (Fig. 15). This region, in comparison with other regions, has the finest hexagonal grid with a size of approximately 173 km, which is close to that of Southern Germany, 150 km. Three series of fine hexagonal patterns are connected at a transportation hub at Atlanta (cf., Fig. 10(b)). The east-bound pattern is directed towards the corridor between the Atlantic Ocean and the Appalachian Mountains, the west-bound one is connected to the hexagonal distribution in the Gulf Coast Region, and the north-bound one is connected to that in the northern industrial district.

The grid around Greenville in Fig. 10(b) looks like a $k = 4$ system based on the *transportation principle* (Christaller, 1933 [10]) in that two important places at Atlanta (B-center) and Charlotte (D-center) are connected by a straight road passing a less important F-center at Greenville. Such a system can also be seen in the triangle between Atlanta (B-center), Nashville (E-center), and Birmingham (E-center), for which three F-centers at Chattanooga, Huntsville, and Anniston are located at the middle points on the sides of the triangle.

T-shaped narrow triangular network in East North Central: In the industrial zone in the East North Central Region (Fig. 9(d)), by the spectrum analysis (Fig. B3), we found one core–satellite pattern and three shifted ones (Fig. 14(b)). These patterns can be assembled into a T-shaped, belt-like, triangular distribu-

tion bordering the Appalachian Mountains and the Great Lakes (Fig. 15). This distribution connects East North Central Region to Atlanta via Nashville and to Washington via the Appalachian Mountains. The average size of the hexagonal grid is approximately 240 km and is significantly greater than that of South Atlantic Region, 173 km.

As shown in Fig. 10(b), the network around Indianapolis looks like a $k = 3$ system based on the *market principle* (Christaller, 1933 [10]) as Indianapolis is located at the center of three large triangular cities: Chicago (B-center), Detroit (C-center), and Cincinnati (D-center). In addition, Nashville at the south border of this region is a hub of city network connecting three regions of the Gulf Coast, the South Atlantic, and the East North Central.

Core–satellite pattern around Kansas City: As shown in Fig. 10, Kansas City (D-center) and surrounding hexagonal F-centers (Columbia, Springfield, Tulsa, Wichita, Omaha, and Des Moines) display a core–satellite pattern, which can be interpreted as a $k = 7$ system based on Christaller’s *administrative principle*.

A line-like distribution in Middle Atlantic: In the Middle Atlantic Region, a line-like distribution of three central places at Boston, New York City, and Washington is observed in a closed narrow corridor between the Atlantic Ocean and the Appalachian Mountains (Figs. 15 and B4).

6. Conclusions

A statistical analysis procedure to detect hexagonal patterns in population centers has been proposed. Although there are mountains and rivers that contradict the basic assumption of a uniform space presumed in central place theory and in this paper, the present analysis was found to be quite robust and capable of systematically detecting self-organizing hexagonal and core-satellite patterns.

The population data of Southern Germany in 2011 were processed by the present procedure and a strong power spectrum for a core–satellite pattern, which looks quite like a hexagonal network, was detected. This confirms the foresight of Christaller, who extracted hexagonal distributions of central places of various sizes in Southern Germany.

The search of hexagonal patterns was extended to Eastern USA, in which a number of cities are spread over a large expanse of flat area. Most of the city subnetworks found herein correspond to core–satellite patterns, while there are a few hexagonal ones. Most of these subnetworks were found to be compatible with each other and are assembled into a gigantic city network encompassing the whole Eastern USA, except for some seaside areas and the Appalachian Mountains. A group-theoretic statistical analysis was useful in the detection of this network with amazing geometrical regularity. An overlapping hexagonal distribution proposed

by Lösch (1940) [35] was observed, while Christaller's $k = 3$, $k = 4$, and $k = 7$ systems were rarely seen (Fig. 10).

The hexagonal and core–satellite patterns are not mere geometrical patterns but serve as possible equilibria that emerge from a uniform state, just as hexagons were envisaged to emerge from an isotropic flat plain in central place theory (Dicken and Lloyd, 1990 [13]). There appears to be an invisible hand in that spatial patterns of possible equilibria emanating from the uniform space also serve as distribution patterns of cities in the real world. The authors would like to recall the book entitled “Fearful Symmetry: Is God a Geometer?,” which describes the geometrical regularity of pattern formation in various physical phenomena (Stewart and Golubitsky, 1992 [47]). Whereas this paper serves as a sociological experiment of pattern formation, the analysis of self-organizing patterns using spatial agglomeration models is a topic to be tackled in the future.

Since cities are complex systems with various aspects, it is vital to overcome complexity to carry out cross-fertilization of the present procedure with other studies of cities, such as empirics and NEG models. It should be emphasized that the present procedure, in principle, is applicable to any spatially distributed scalar properties for economic activity and their time evolution.

For the 18×18 hexagonal lattice, there are as many as 324 potential spectra.

Nonetheless, these 324 spectra were decomposed into 37 subsets associated with self-organizing bifurcating patterns from a uniform state. Moreover, through the application of the present spectrum analysis, we have noted that the variety of dominant spectra is quite limited. Among the 19 city networks found in this paper, there was a single network for each of the three hexagons, four hexagons, and nine hexagons, whereas the remaining 16 city networks were all core–satellite patterns. This fact implies that, at the least for the city population analysis, it is possible to reduce the number of potential spectra expressing the spatial agglomeration patterns based on the present spectrum analysis. In addition, knowledge of the spatial patterns suggests plausible spatial platforms for spatial economy models.

This paper employed a hexagonal lattice as a spatial platform but does not deny the possibility of other spatial platforms. For example, Eaton and Lipsey (1976) [16] demonstrated for a simple economic model that there is a wide range of configurations of firms—including squares, regular triangles, and so on. A square lattice, which is more widely used in the studies of spatial agglomeration (Footnote 9), would be a possible alternative for a spatial platform. It will be a topic in the future to compare the performance of square and hexagonal lattices.

References

- [1] Batty, Michael. 2008. “The size, scale, and shape of cities,” *Science*, 319, 769–771.
- [2] ———. 2013. *The New Science of Cities*, MIT Press, Cambridge.
- [3] Batty, Michael and Paul Longley. 1994. *Fractal Cities*, Academic Press, San Diego.
- [4] Bettencourt, Luis M. A. 2013. “The origins of scaling in cities,” *Science*, 340(6139), 1438–1441.
- [5] Bitner, Agnieszka, Robert Hołyst, and Marcin Fiałkowski. 2009. “From complex structures to complex processes: Percolation theory applied to the formation of a city,” *Physical Review E*, 80(4), 037102-1–4.
- [6] Black, Duncan and Vernon Henderson. 2003. “Urban evolution in the USA,” *Journal of Economic Geography*, 3(4), 343–372.
- [7] Bosker, Maarten, Steven Brakman, Harry Garretsen, and Marc Schramm. 2008. “A century of shocks: The evolution of the German city size distribution 1925–1999,” *Regional Science and Urban Economics*, 38(4), 330–347.

- [8] ———. 2010. “Adding geography to the new economic geography: bridging the gap between theory and empirics,” *Journal of Economic Geography*, 10(6), 793–823.
- [9] Brakman, Steven, Harry Garretsen, Charles van Marrewijk, and Marianne van den Berg. 1999. “The return of Zipf: Towards a further understanding of the rank-size distribution,” *Journal of Regional Science*, 39(1), 183–213.
- [10] Christaller, Walter. 1933. *Die zentralen Orte in Süddeutschland*. Gustav Fischer, Jena. English translation: 1966. *Central Places in Southern Germany*. Prentice Hall, Englewood Cliffs.
- [11] Clarke, Martin and Alan G. Wilson. 1983. “The dynamics of urban spatial structure: Progress and problems,” *Journal of Regional Science*, 23(1), 1–18.
- [12] Davies, Paul S., Michael J. Greenwood, and Haizheng Li. 2001. “A conditional logit approach to U.S. state-to-state migration,” *Journal of Regional Science*, 41(2), 337–360.
- [13] Dicken, Peter and Peter E. Lloyd. 1990. *Location in Space: Theoretical Perspectives in Economic Geography*, 3rd ed., Harper Collins.

- [14] Duranton, Gilles. 2006. "Some foundations for Zipf's law: Product proliferation and local spillovers," *Regional Science and Urban Economics*, 36, 542–563.
- [15] Eaton, B. Curtis and Richard G. Lipsey. 1975. "The principle of minimum differentiation reconsidered: some new developments in the theory of spatial competition," *The Review of Economic Studies*, 42(1), 27–49.
- [16] ——. 1976. "The non-Uniqueness of equilibrium in the Löschian location model," *American Economic Review*, 66(1), 71–93.
- [17] ——. 1982. "An economic theory of central places," *The Economic Journal*, 92(365), 56–72.
- [18] Findeisena, Sebastian and Jens Südekum. 2008. "Industry churning and the evolution of cities: Evidence for Germany," *Journal of Urban Economics*, 64(2), 326–339.
- [19] Forslid, Rikard and Gianmarco I. P. Ottaviano. 2003. "An analytically solvable core-periphery model," *Journal of Economic Geography*, 3, 229–340.
- [20] Fujita, Masahisa, Paul Krugman, and Tomoya Mori. 1999. "On the evo-

- lution of hierarchical urban systems,” *European Economic Review*, 43(2), 209–251.
- [21] Gabaix, Xavier. 1999. “Zipf’s law for cities: An explanation,” *The Quarterly Journal of Economics*, 114(3), 739–767.
- [22] Golubitsky, Martin and Ian Stewart. 2002. *The Symmetry Perspective: From Equilibrium to Chaos in Phase Space and Physical Space*, Birkhäuser, Basel.
- [23] Golubitsky, Martin, Ian Stewart, and David G. Schaeffer. 1988. *Singularities and Groups in Bifurcation Theory*, Vol. 2, Springer-Verlag, New York.
- [24] Gonzalez-Val, Rafael. 2010. “The evolution of U.S. city size distribution from a long-term perspective (1900–2000),” *Journal of Regional Science*, 50(5), 952–972.
- [25] Hsu, Wen-Tai, Tomoya Mori, and Tony E. Smith. 2014. “Spatial patterns and size distributions of cities,” *KIER Discussion Paper Series*, 882.
- [26] Ikeda, Kiyohiro and Kazuo Murota. 2014. *Bifurcation Theory for Hexagonal Agglomeration in Economic Geography*, Springer-Verlag, Tokyo.

- [27] Ikeda, Kiyohiro, Kazuo Murota, and Takashi Akamatsu. 2012. “Self-organization of Lösch’s hexagons in economic agglomeration for core–periphery models,” *International Journal of Bifurcation and Chaos*, 22(8), 1230026-1–1230026-29.
- [28] Ikeda, Kiyohiro, Kazuo Murota, Takashi Akamatsu, Tatsuhito Kono, and Yuki Takayama. 2014. “Self-organization of hexagonal agglomeration patterns in new economic geography models,” *Journal of Economic Behavior & Organization*, 99, 32–52.
- [29] Ikeda, Kiyohiro, Kazuo Murota, and Yuki Takayama. 2017. “Stable economic agglomeration patterns in two dimensions: beyond the scope of central place theory,” *Journal of Regional Science*, 57(1), 132–172.
- [30] Ioannides, Yannis M., Henry G. Overman. 2004. “Spatial evolution of the US urban system,” *Journal of Economic Geography*, 4 (2), 131–156.
- [31] Kim, Sukkou. 2007. “Changes in the nature of urban spatial structure in the United States, 1890–2000,” *Journal of Regional Science*, 47(2), 273–287.
- [32] Koschmieder, E. Lothar. 1993. *Benard Cells and Taylor Vortices*, Cambridge University Press, Cambridge.

- [33] Krugman, Paul. 1993. "On the number and location of cities," *European Economic Review*, 37, 293–298.
- [34] ———, 1996. *The Self-Organizing Economy*, Blackwell, Oxford.
- [35] Lösch, August. 1940. *Die räumliche Ordnung der Wirtschaft*, Gustav Fischer, Jena. English translation: 1954. *The Economics of Location*, Yale University Press, New Haven.
- [36] Makse, Hernán A., Shlomo Havlin, and H. Eugene Stanley. 1995. "Modelling urban growth patterns," *Nature*, 377, 608–612.
- [37] Mori, Tomoya and Tony E. Smith. 2011 "An industrial agglomeration approach to central place and city size regularities," *Journal of Regional Science*, 51(4), 694–731.
- [38] Mulligan, Gordon F., Mark D. Partridge, and John I. Carruthers. 2012. "Central place theory and its reemergence in regional science," *The Annals of Regional Science*, 48(2), 405–431.
- [39] Munz, Martin and Wolfgang Weidlich. 1990. "Settlement formation, Part II: Numerical simulation," *The Annals of Regional Science*, 24, 177–196.

- [40] NASA Earth Observatory of USA taken by the Suomi NPP satellite (2012):
<http://earthobservatory.nasa.gov/NaturalHazards/view.php?id=79800>
- [41] Overman, Henry G., Yannis M. Ioannides. 2001. “Cross sectional evolution of the U.S. city size distribution,” *Journal of Urban Economics*, 49, 543–566.
- [42] Partridge, Mark D., Dan S. Rickman, Kamar Ali, M. Rose Olfert. 2008. “Lost in space: population growth in the American hinterlands and small cities,” *Journal of Economic Geography*, 8(6), 727–757.
- [43] Redding, Stephen J. and Daniel M. Sturm. 2008. “The costs of remoteness: Evidence from German division and reunification,” *The American Economic Review*, 98(5), 1766–1797.
- [44] Rossi-Hansberg, Esteban and Mark L. J. Wright. 2007. “Urban structure and growth. *The Review of Economic Studies*, 74, 597–624.
- [45] Sanglier, Michèle and Peter Allen. 1989. “Evolutionary models of urban systems: an application to the Belgian provinces,” *Environment and Planning A* 21, 477–498.

- [46] Stelder, Dirk. 2005. "Where do cities form? A geographical agglomeration model for Europe," *Journal of Regional Science*, 45, 657–679.
- [47] Stewart, Ian and Martin Golubitsky 1992. *Fearful Symmetry: Is God a Geometer?* Blackwell, Oxford.
- [48] Weidlich, Wolfgang. 2000. *Sociodynamics*, Dover, Mineola, New York.
- [49] Weidlich, Wolfgang and Günter Haag. 1987. "A dynamic phase transition model for spatial agglomeration processes," *Journal of Regional Science*, 27(4), 529–569.
- [50] Zipf, George K. 1949. *Human Behavior and the Principle of Least Effort*, Addison Wesley, Cambridge.

Table 1: The size D of a hexagon and the number $M(m)$ of basis vectors labeled by $m \in L_{\text{hexa}}$ for $n = 18$.

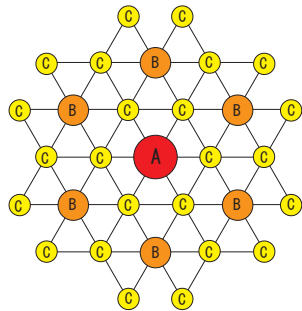
m	D	$M(m)$	m	D	$M(m)$
1	1	1	36(II)	36	12
3	3	2	81(I), 81(II), 81(III)	81	6
4	4	3	81(IV), 81(V), 81(VI)	81	12
9	9	6	108(I), 108(II), 108(III)	108	6
12	12	6	108(IV), 108(V), 108(VI)	108	12
27(I), 27(II), 27(III)	27	6	324(I), 324(II), 324(III)	324	6
36(I)	36	6	324(IV), 324(V), ..., 324(XV)	324	12

Table 2: Original sources of population data.

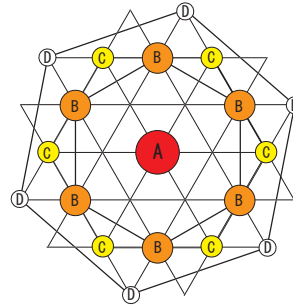
Country	Data bank (Date, Type) and Internet address
Germany	Statistisches Bundesamt Deutschland (1987/5/25, Census; 2001/12/31, Estimate; 2011/05/09, Census) https://www.destatis.de/EN/Homepage.html
Austria	Statistik Austria (1991/5/15, 2001/5/15, 2011/10/31, Census) http://www.statistik.at/web_de/statistiken/index.html
France	Institut National de la Statistique et des Études Économiques (1990/3/5, 1999/3/8, Census; 2012/01/01, Estimate) http://www.insee.fr/fr/
Switzerland	Swiss Statistics (1990/12/4, 2000/12/5, 2010/12/31, Census) http://www.bfs.admin.ch/bfs/portal/en/index.html
Luxembourg	Le Portail des Statistiques du Luxembourg (1991/3/1, 2001/2/15, 2011/02/01, Census) http://www.statistiques.public.lu/en/index.html
USA	US Census Bureau (2014/07/01, Estimate) http://www.census.gov/
Canada	Statistics Canada (2014/07/01, Estimate) http://www.statcan.gc.ca/start-debut-eng.html

Table 3: City population size classification for the cities in Fig. 6(c) (city population is based on administrative division).

Name of center	Name of City	Population
A-center ($\lambda \geq 1,000,000$)	Canton of Zürich	1,373,068
	München Stadt	1,348,335
B-center ($500,000 \leq \lambda < 1,000,000$)	Frankfurt am Main	667,925
	Stuttgart	585,890
C-center ($300,000 \leq \lambda < 500,000$)	Nürnberg	486,314
	Strasbourg	482,384
	Mulhouse	349,764
	Stadtverband Saarbrücken	327,065
D-center ($\lambda < 300,000$)	Konstanz	266,964
	Basel-Stadt	184,950



(a) A distribution of Christaller



(b) Three overlapping smallest hexagons of Lösch

Figure 1: Hexagonal distributions of Christaller and Lösch. A larger circle expresses a larger place.



Figure 2: City lights of USA taken by Suomi NPP satellite (NASA, 2012 [40]). This image of the United States of America at night is a composite assembled from data acquired by the Suomi NPP satellite in April and October 2012.

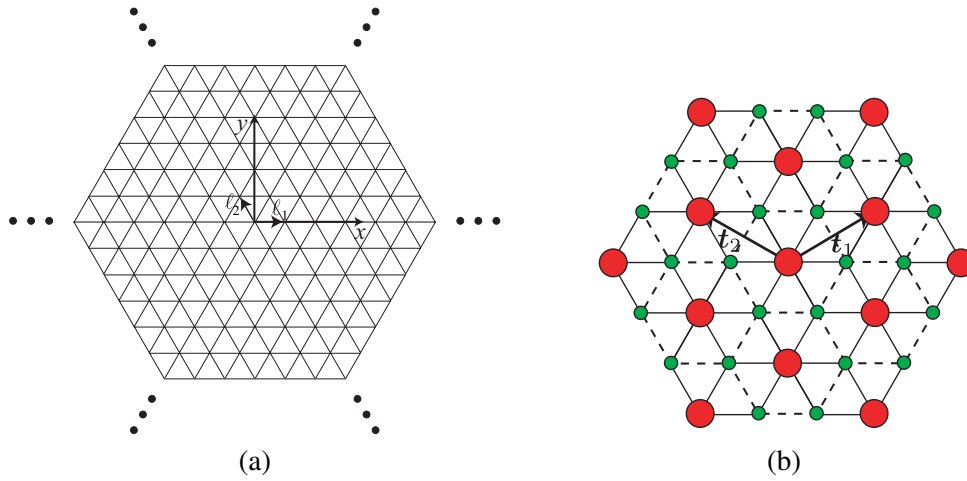


Figure 3: (a) Hexagonal lattice. (b) A hexagonal distribution for $(\alpha, \beta) = (2, 1)$.

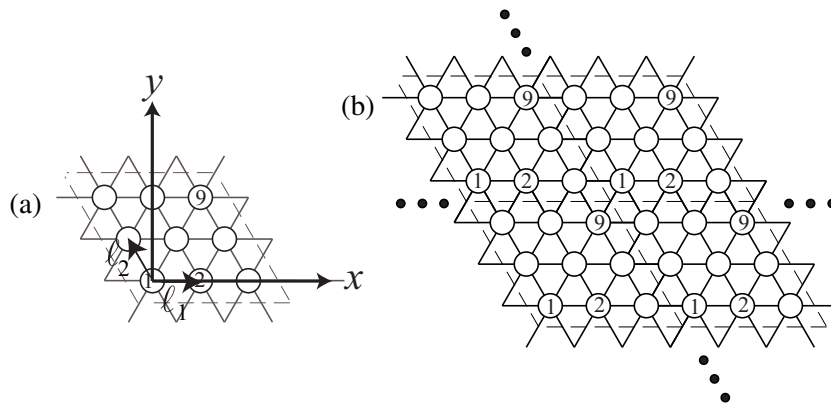


Figure 4: A system of places on a hexagonal lattice with periodic boundary conditions. (a) 3×3 hexagonal lattice. (b) Spatially repeated 3×3 hexagonal lattices using periodic boundary conditions.

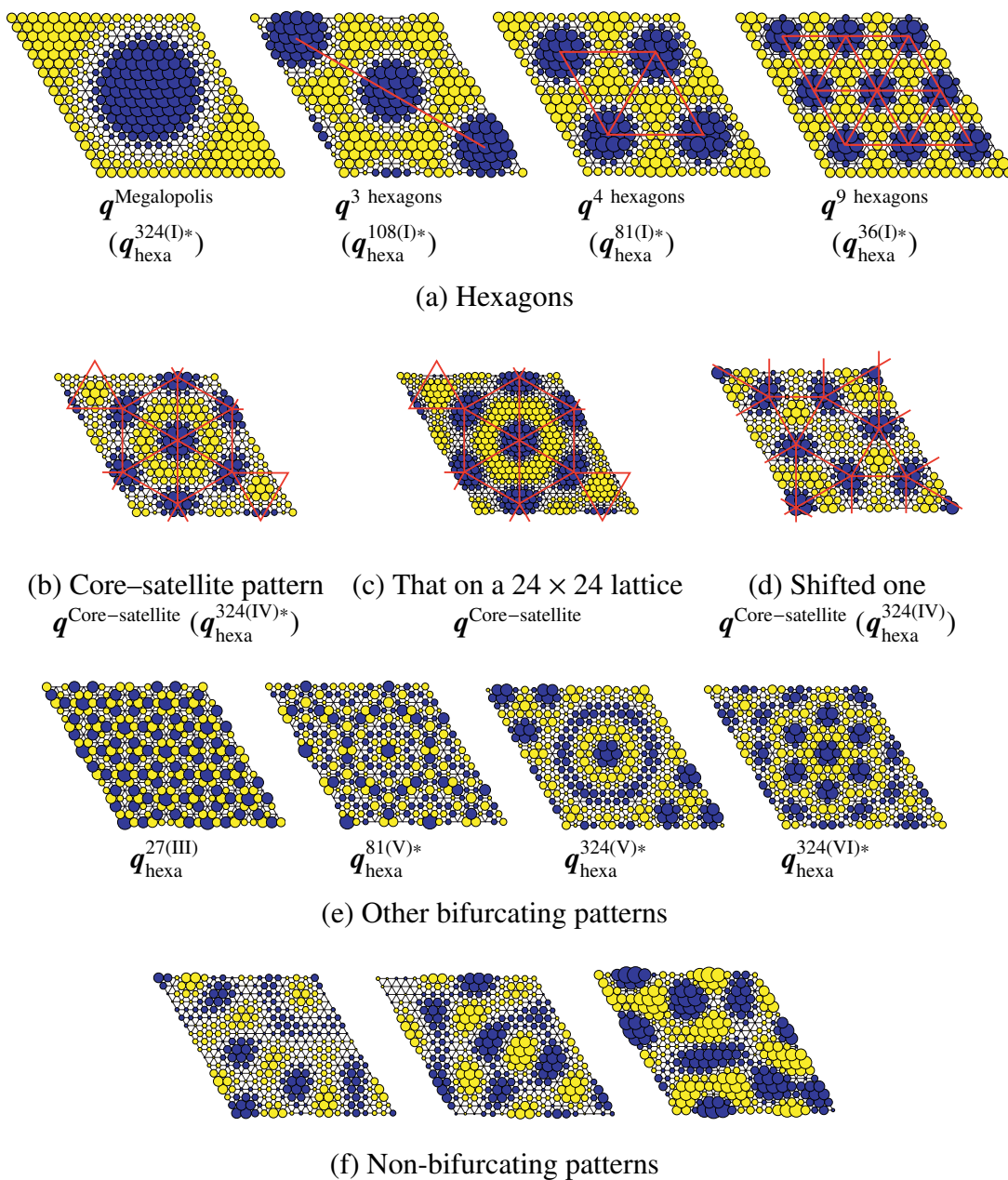


Figure 5: Patterns appearing on an 18×18 hexagonal lattice expressed by $q^{(m)}$. Hexagons centered at $(n_1, n_2) = (9, 9)$ are expressed by $q_{\text{hexa}}^{(m)*}$; a blue circle denotes a positive component, a yellow circle indicates a negative one, the area of a circle expresses the magnitude of the component, and a red line is used to clarify spatial patterns.

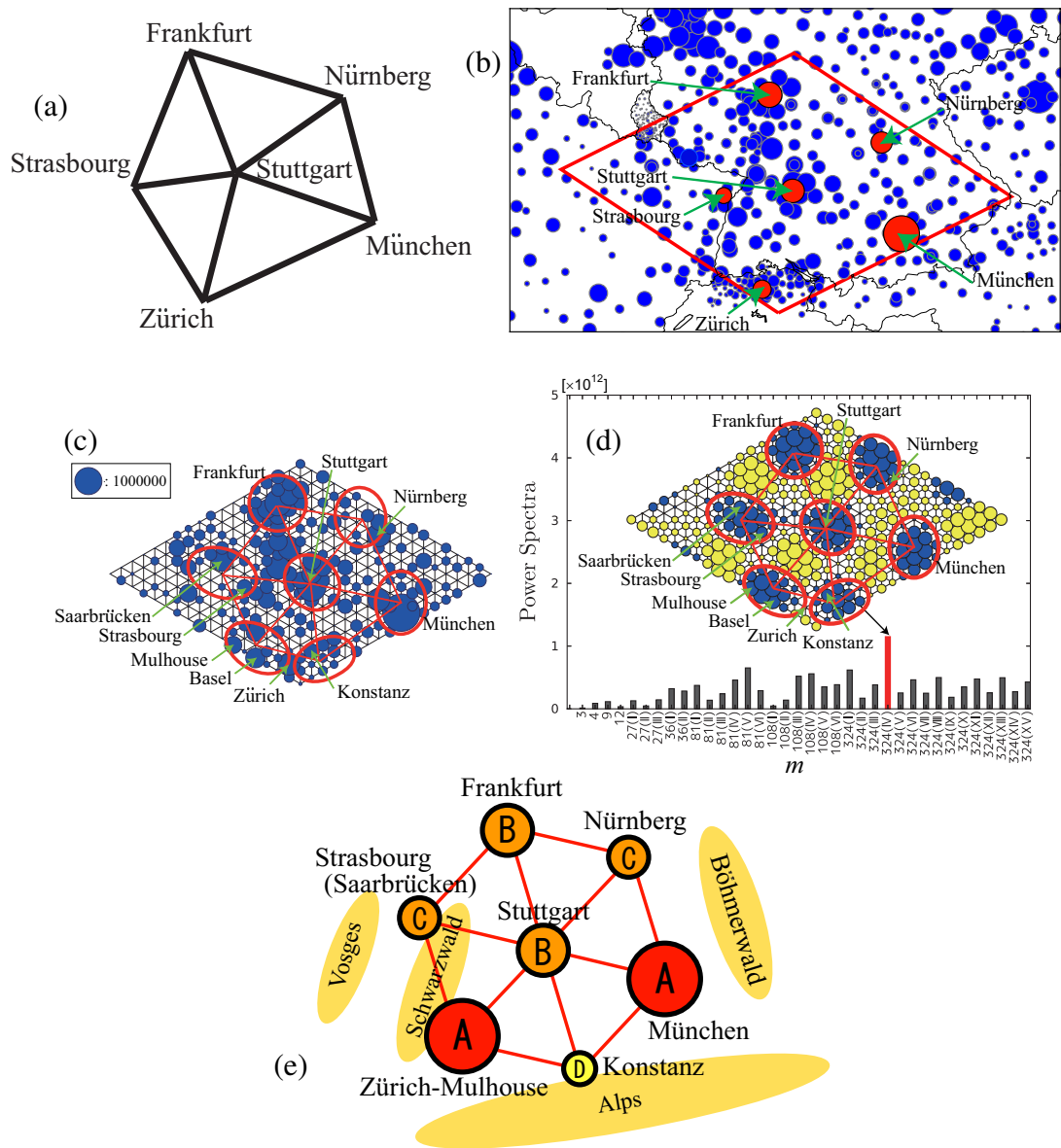
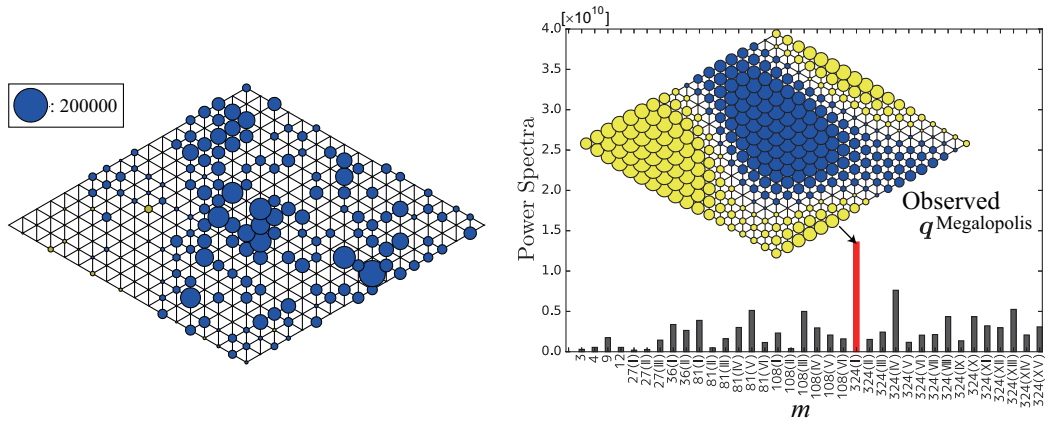
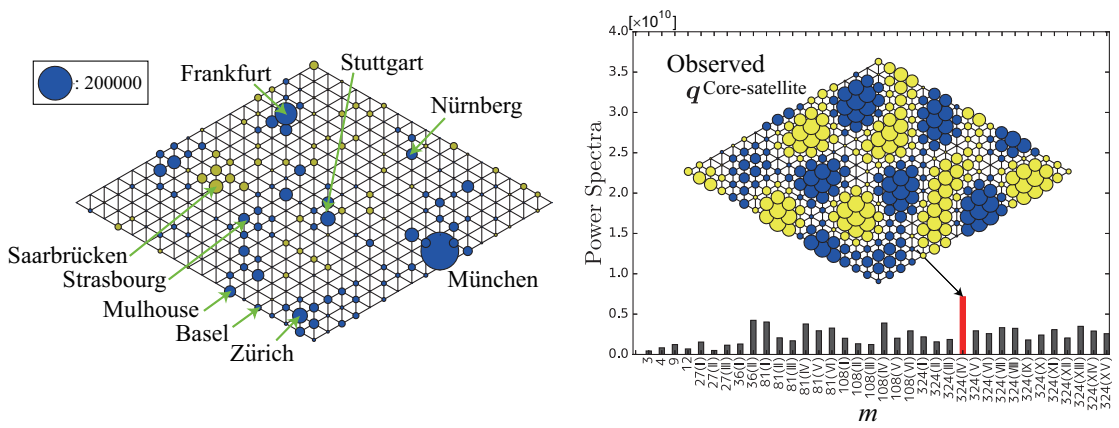


Figure 6: (a) Christaller's pentagonal distribution of cities (Christaller, 1966, p.224–225 [10]). (b) The domain used for the spectrum analysis of the population of Southern Germany and neighboring countries. The area of a circle denotes the population size. (c) Population map and circular or elliptic zones of agglomeration on an 18×18 hexagonal lattice. A series of red lines denotes the distribution of cities. (d) Power spectra of the squared magnitudes $\|q^{(m)}\|^2$ of the assembled Fourier terms and the spatial pattern of the largest spectrum $q^{\text{Core-satellite}}$. The area of a blue circle in this pattern denotes the increase of population and that of a yellow one denotes its decrease. (e) Interpretation of a distribution of cities.

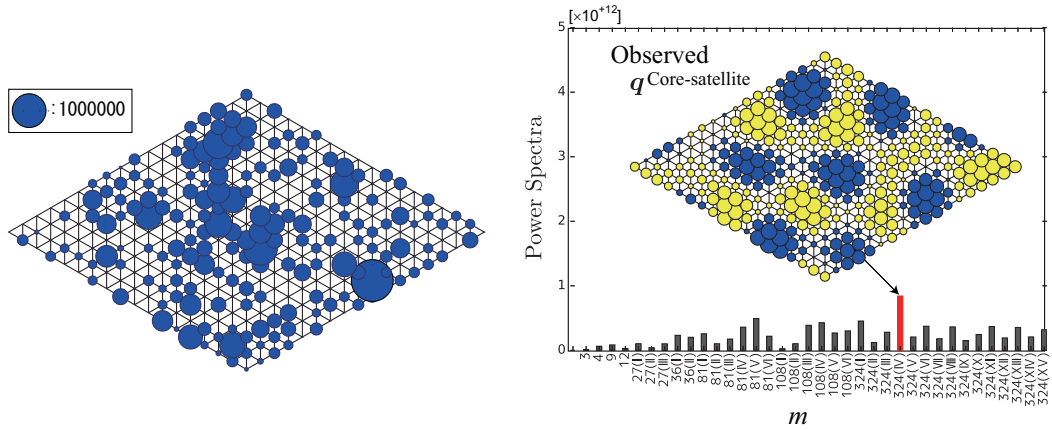


(a) 1987–2000

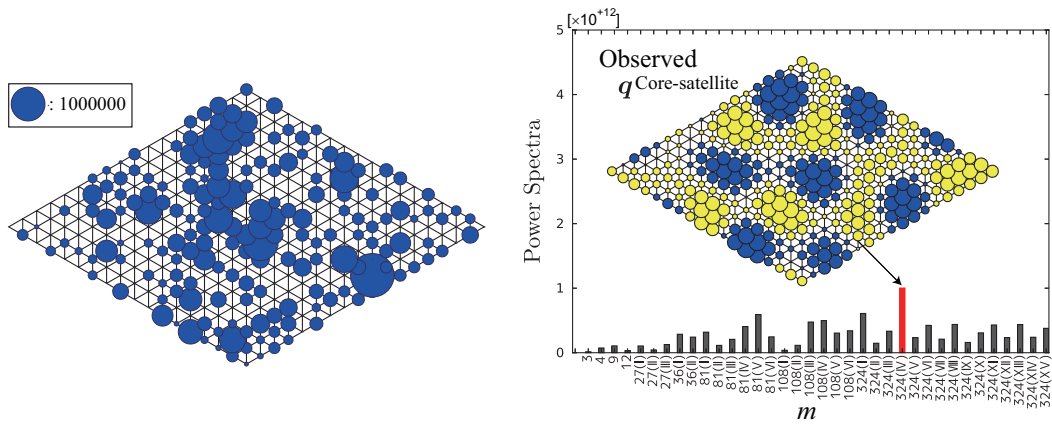


(b) 2000–2011

Figure 7: Time evolution of the spectra of the population increment between 1987 to 2011 in Southern Germany. A blue circle denotes a positive component, a yellow circle indicates a negative one, and the area of a circle expresses the magnitude of the component.



(a) 1987



(b) 2000

Figure 8: Time cross-sectional views of the spectra of the population in 1987 and 2011 in Southern Germany. The area of a circle expresses the magnitude of the component.

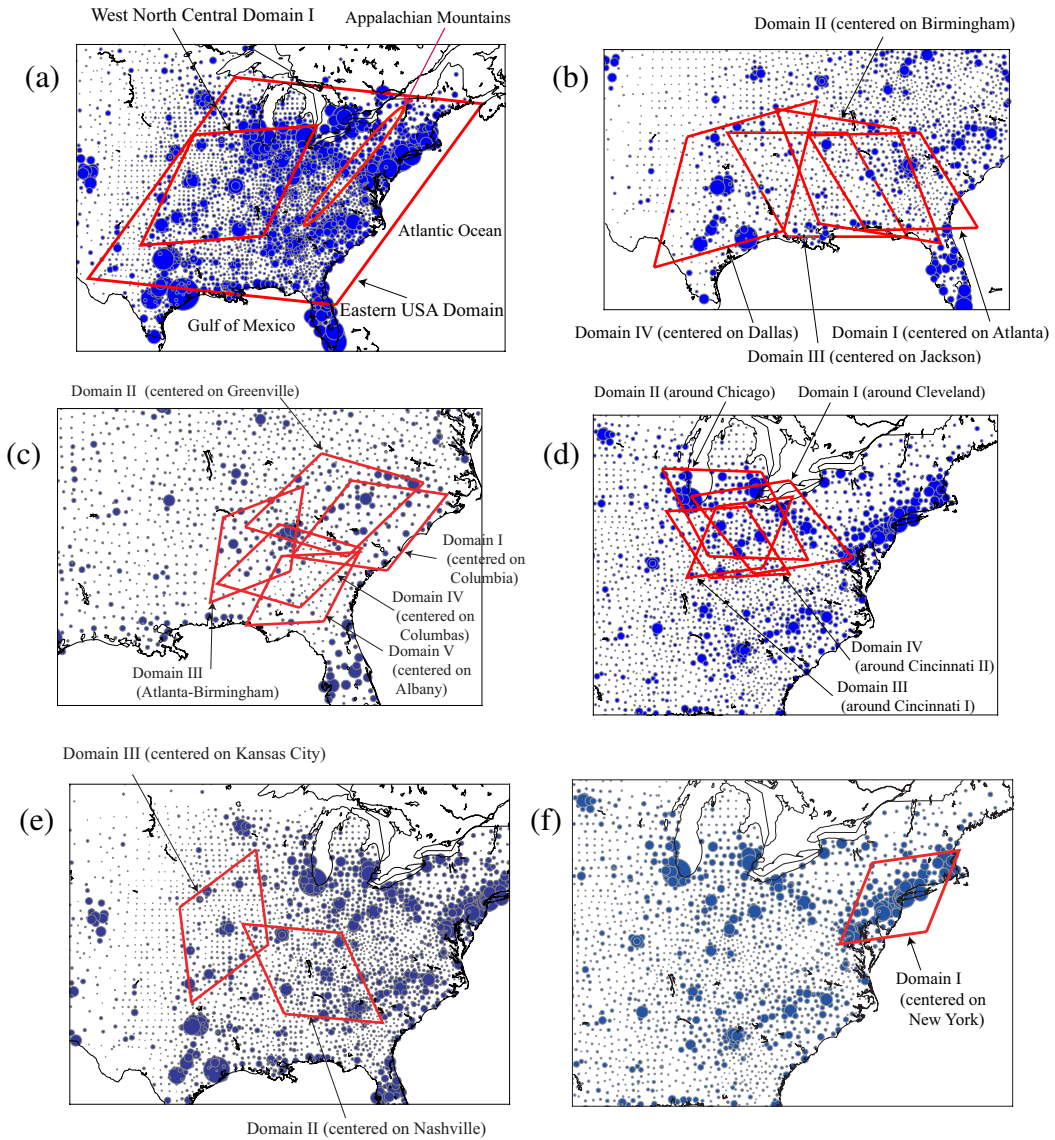


Figure 9: Rhombic domains for the spectrum analysis drawn on population maps in Eastern USA. (a) Eastern USA Domain and West North Central Domain I. (b) Gulf Coast Region (Domains I–IV). (c) South Atlantic Region (Domains I–V). (d) East North Central Region (Domains I–IV). (e) West North Central Region (Domains II–III). (f) Middle Atlantic Region (Domain I).

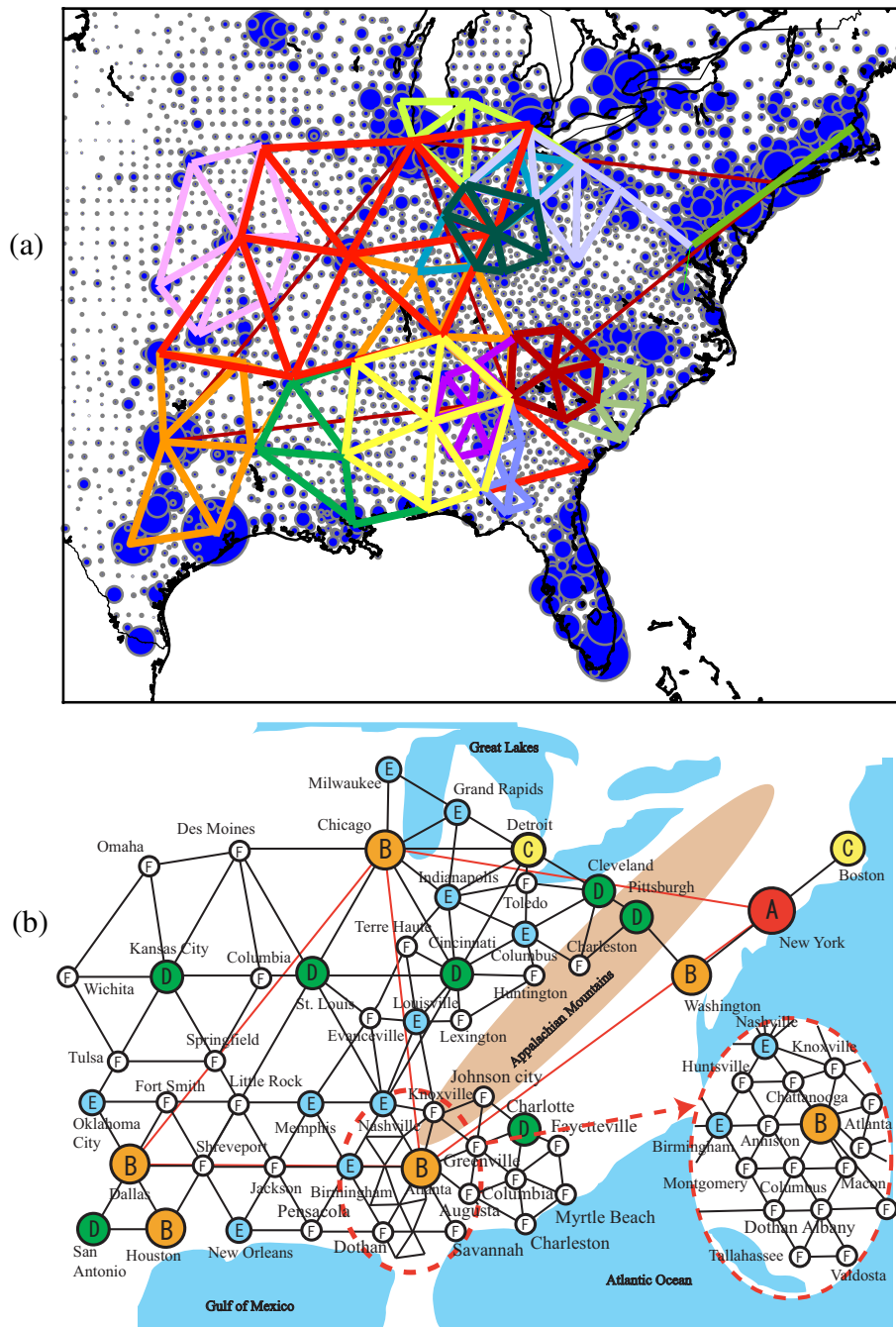


Figure 10: (a) Assembled distribution of cities in Eastern USA drawn on a population map. The area of a circle denotes the population size and lines with different colors indicate city sub-distributions. (b) Interpretation of the distribution of cities in Eastern USA. Cities are classified from A-center to F-center (Table B1).

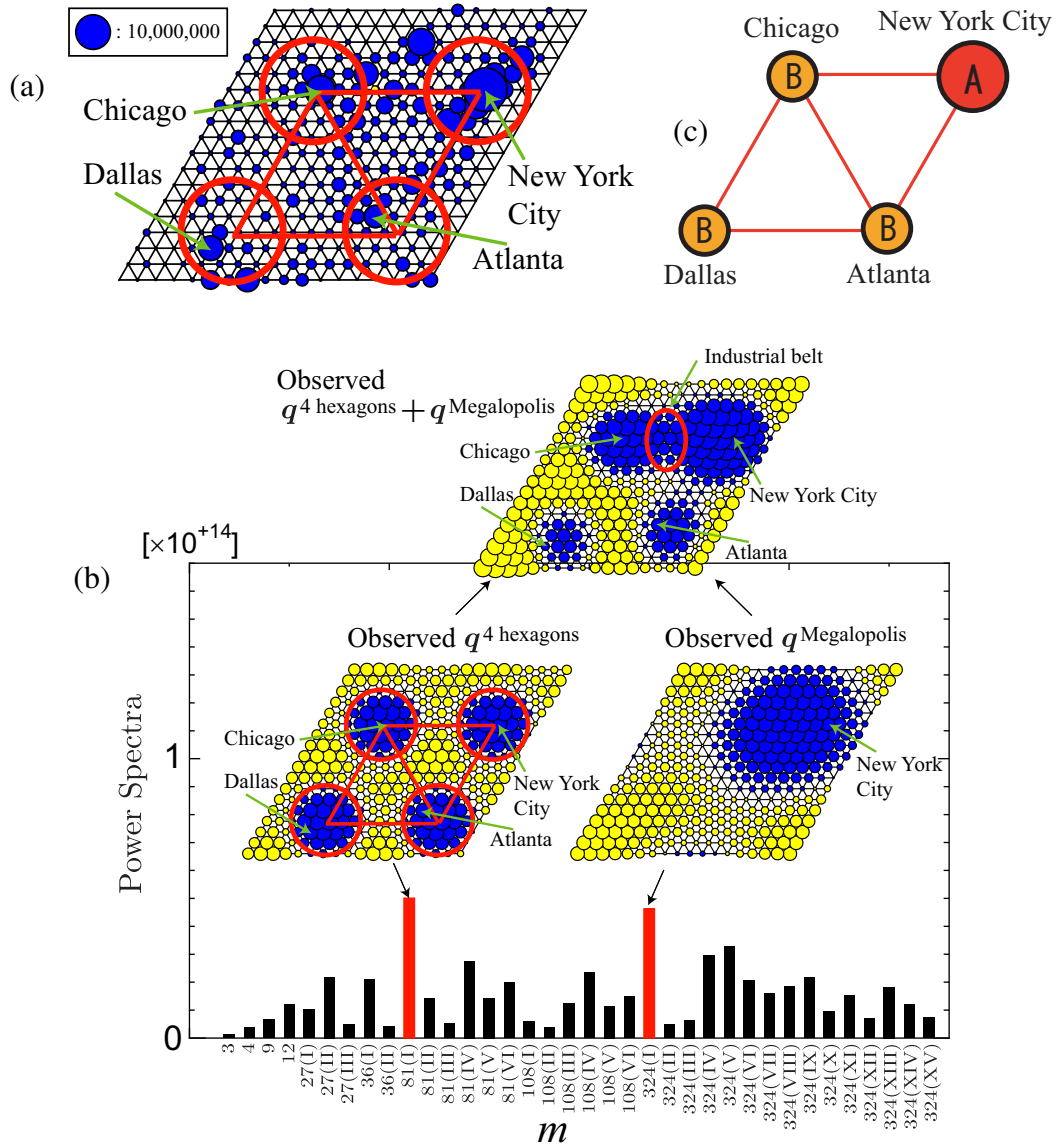


Figure 11: Spectrum analysis for Eastern USA Domain. (a) Discretized population map and a distribution of cities. The area of a blue circle denotes the population size and a series of red lines denotes the distribution of cities. (b) Power spectra of the squared magnitudes $\|q^{(m)}\|^2$ of the assembled Fourier terms and spatial patterns of the predominant spectra q^4 hexagons and q Megalopolis for this region. A blue circle denotes a positive component, a yellow circle indicates a negative one, and the area of a circle expresses the magnitude of the component. (c) Interpretation of distribution of cities.

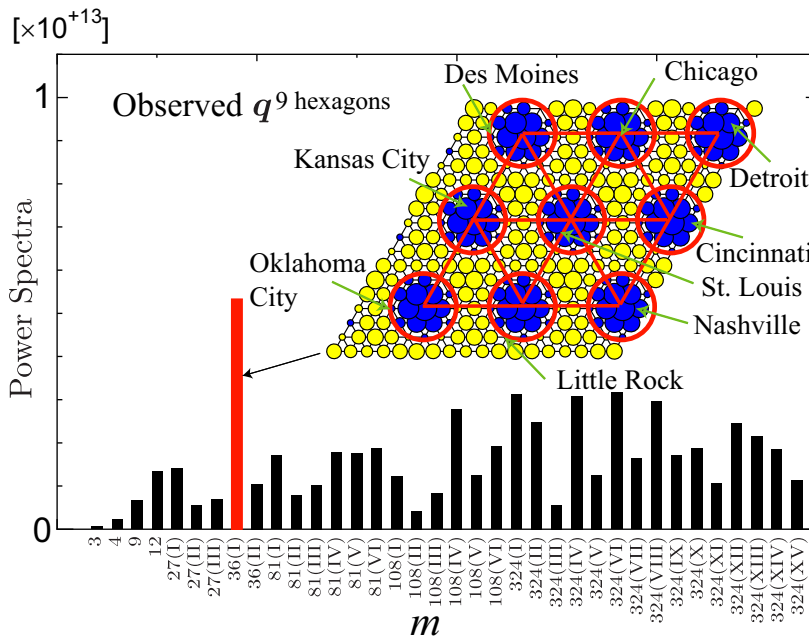
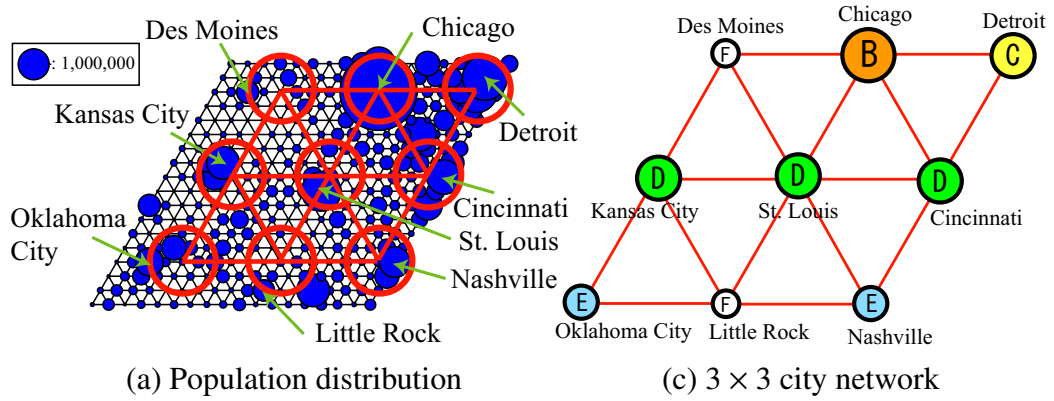


Figure 12: Spectrum analysis for West North Central Region centered on St. Louis. (a) Discretized population map and a distribution of cities. The area of a blue circle denotes the population size and a series of red lines denotes the distribution of cities. (b) Power spectra of the squared magnitudes $\|q^{(m)}\|^2$ of the assembled Fourier terms and the spatial pattern of the predominant spectrum $q^{9\text{hexagons}}$ for this region. The area of a blue circle of this pattern denotes an increase of population and that of a yellow one denotes a decrease; a series of red lines denotes the distribution of cities. (c) Interpretation of distribution of cities.

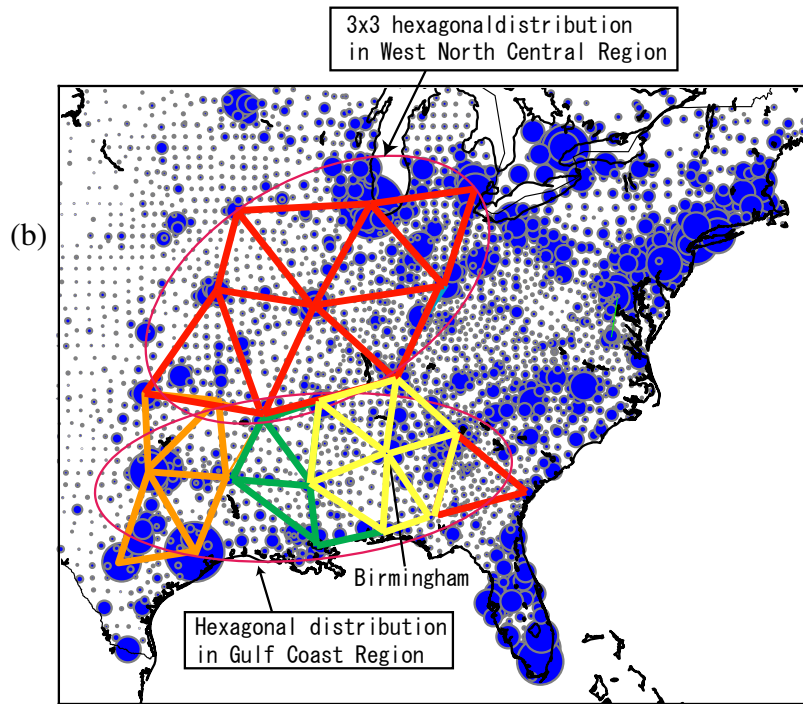
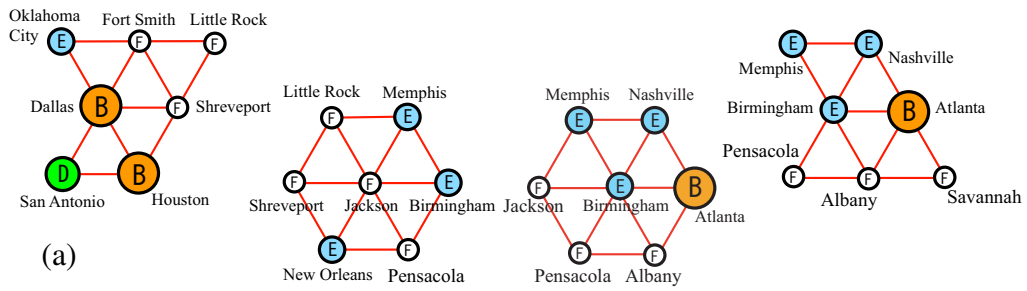


Figure 13: Clearest hexagonal distributions of cities in Gulf Coast Region. (a) Interpretation of distributions of cities. (b) Assembled distributions of cities for West North Central and Gulf Coast Regions.

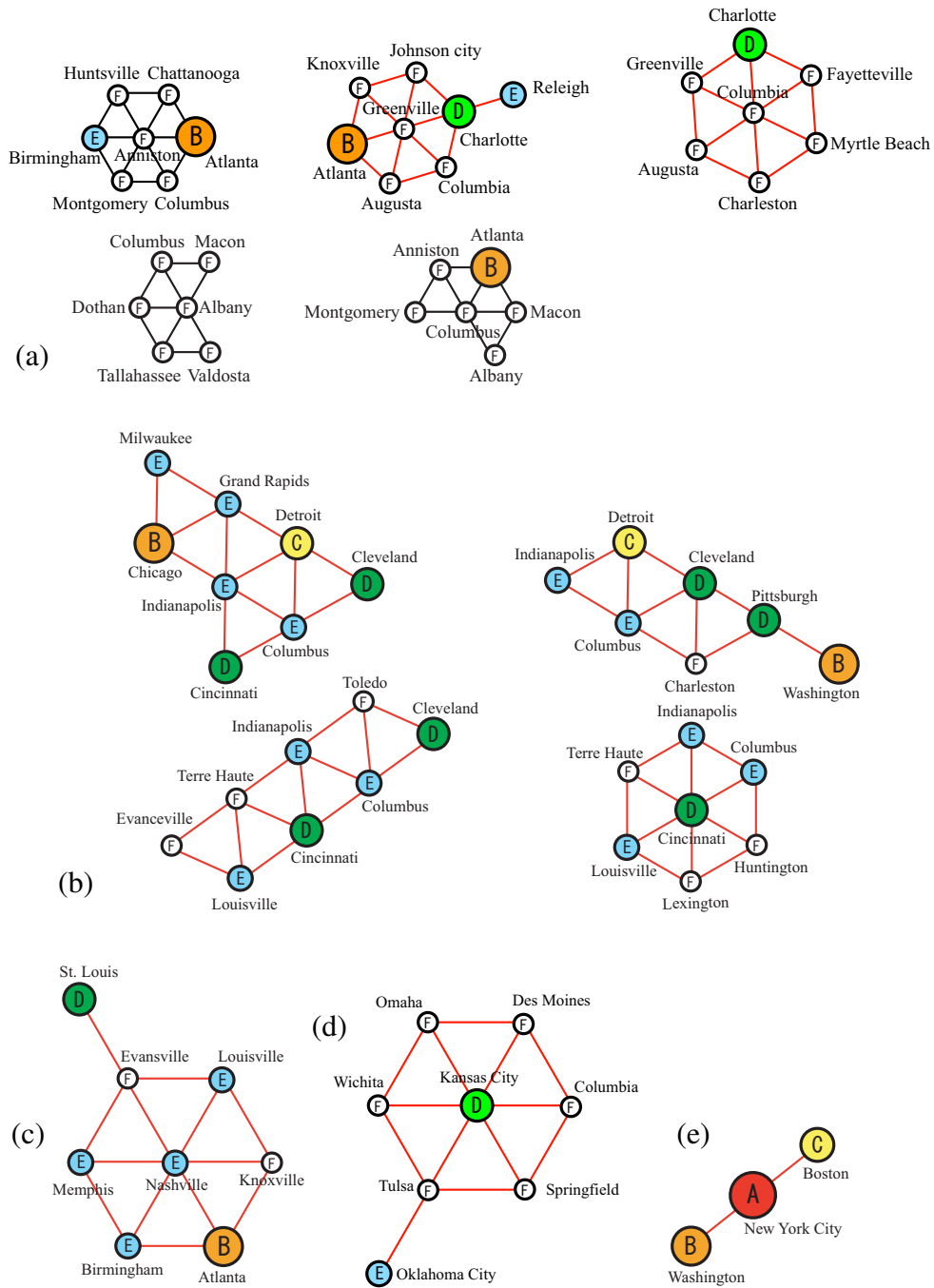


Figure 14: Interpretation of distributions of cities in other regions. (a) South Atlantic Region. (b) East North Central Region. (c) West North Central Domain II. (d) West North Central Domain III. (e) Middle Atlantic Region.

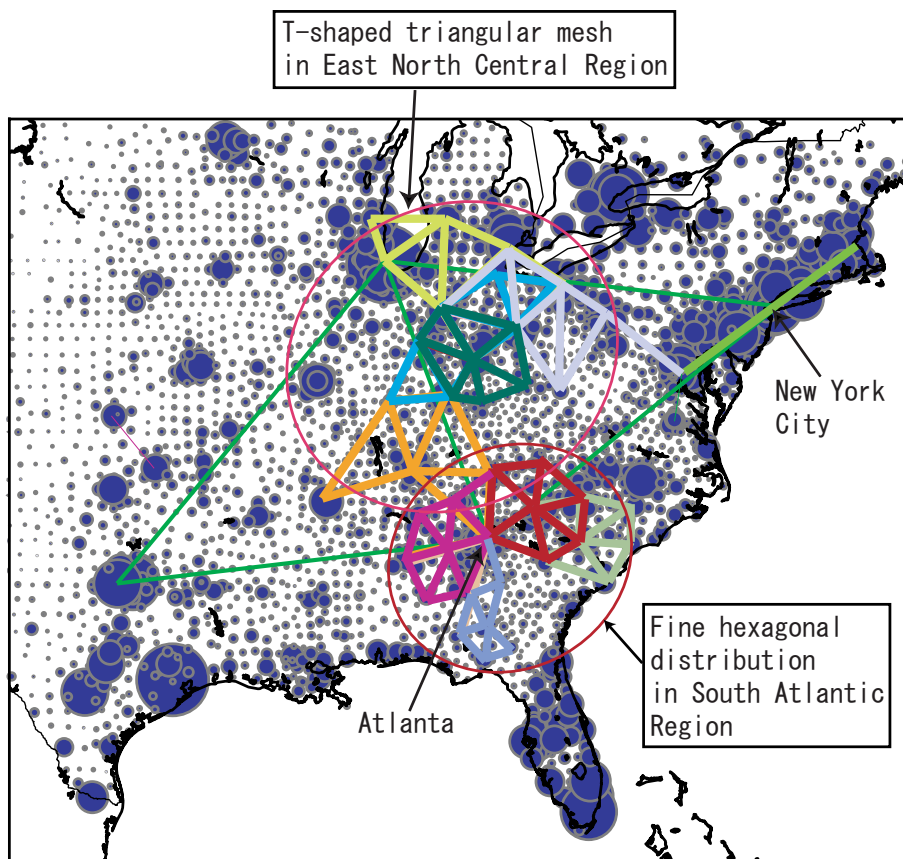


Figure 15: Distributions of cities in East North Central, South Atlantic, and Middle Atlantic Regions.

A. Group-theoretic double Fourier series and associated spatial patterns

We present a group-theoretic double Fourier series for the 18×18 hexagonal lattice that is used in the present spectrum analysis. The basis vectors of this lattice can be decomposed into several subsets which represent patterns with hexagonal symmetry of various kinds.

The rearranged double Fourier series for the 18×18 hexagonal lattice is presented Ikeda and Murota (2014) [26]. The coordinate of a place on the $n \times n$ hexagonal lattice is given by

$$\mathbf{x} = n_1 \boldsymbol{\ell}_1 + n_2 \boldsymbol{\ell}_2, \quad (n_1, n_2 = 0, 1, \dots, n-1),$$

and the places are indexed by (n_1, n_2) . Accordingly, the population distribution vector is indexed as $\boldsymbol{\lambda} = (\lambda_{n_1 n_2} \mid n_1, n_2 = 0, \dots, n-1)$. For a vector $(g(n_1, n_2) \mid n_1, n_2 = 0, 1, \dots, n-1)$ on the lattice with $g(n_1, n_2)$ being the (n_1, n_2) -component, we use the notation $\langle g(n_1, n_2) \rangle$ for its normalization ($n = 18$):

$$\langle g(n_1, n_2) \rangle = (g(n_1, n_2) / (\sum_{i=0}^{n-1} \sum_{j=0}^{n-1} g(i, j)^2)^{1/2} \mid n_1, n_2 = 0, 1, \dots, n-1).$$

First, the basis vectors $\mathbf{q}_1^{(m)}, \dots, \mathbf{q}_{M(m)}^{(m)}$ for $m = 1, 3$ and 4 are given by

$$\begin{aligned} \mathbf{q}_1^{(1)} &= \frac{1}{6}(1, \dots, 1)^\top, \\ [\mathbf{q}_1^{(3)}, \mathbf{q}_2^{(3)}] &= [\langle \cos(2\pi(n_1 - 2n_2)/3) \rangle, \langle \sin(2\pi(n_1 - 2n_2)/3) \rangle], \\ [\mathbf{q}_1^{(4)}, \mathbf{q}_2^{(4)}, \mathbf{q}_3^{(4)}] &= [\langle \cos(\pi n_1) \rangle, \langle \cos(\pi n_2) \rangle, \langle \cos(\pi(n_1 - n_2)) \rangle]. \end{aligned}$$

The basis vectors for $m = 9, 36(\text{I}), 81(\text{I}), 81(\text{II}), 81(\text{III}), 324(\text{I}), 324(\text{II}),$ and $324(\text{III})$ are given by

$$\begin{aligned} \left[\mathbf{q}_1^{(m)}, \dots, \mathbf{q}_6^{(m)} \right] = & \left[\langle \cos(2\pi k n_1/n) \rangle, \langle \sin(2\pi k n_1/n) \rangle, \right. \\ & \langle \cos(2\pi k(-n_2)/n) \rangle, \langle \sin(2\pi k(-n_2)/n) \rangle, \\ & \left. \langle \cos(2\pi k(-n_1 + n_2)/n) \rangle, \langle \sin(2\pi k(-n_1 + n_2)/n) \rangle \right] \end{aligned}$$

with $n = 18$ and the correspondence

m	9	36(I)	81(I)	81(II)	81(III)	324(I)	324(II)	324(III)
k	6	3	2	4	8	1	5	7

The basis vectors for $m = 12, 27(\text{I}), 27(\text{II}), 27(\text{III}), 108(\text{I}), 108(\text{II}),$ and $108(\text{III})$ are given by

$$\begin{aligned} \left[\mathbf{q}_1^{(m)}, \dots, \mathbf{q}_6^{(m)} \right] = & \left[\langle \cos(2\pi k(n_1 + n_2)/n) \rangle, \langle \sin(2\pi k(n_1 + n_2)/n) \rangle, \right. \\ & \langle \cos(2\pi k(n_1 - 2n_2)/n) \rangle, \langle \sin(2\pi k(n_1 - 2n_2)/n) \rangle, \\ & \left. \langle \cos(2\pi k(-2n_1 + n_2)/n) \rangle, \langle \sin(2\pi k(-2n_1 + n_2)/n) \rangle \right] \end{aligned}$$

with the correspondence

m	12	27(I)	27(II)	27(III)	108(I)	108(II)	108(III)
k	3	2	4	8	1	5	7

The basis vectors for $m = 12, 36(\text{II}), 81(\text{IV}), 81(\text{V}), 81(\text{VI}), 108(\text{IV}), 108(\text{V}), 108(\text{VI}), 324(\text{IV}), \dots, 324(\text{XV})$ are given by

$$\begin{aligned} \left[\mathbf{q}_1^{(m)}, \dots, \mathbf{q}_{12}^{(m)} \right] = & \left[\langle \cos(2\pi(kn_1 + \ell n_2)/n) \rangle, \langle \sin(2\pi(kn_1 + \ell n_2)/n) \rangle, \right. \\ & \langle \cos(2\pi(\ell n_1 - (k + \ell)n_2)/n) \rangle, \langle \sin(2\pi(\ell n_1 - (k + \ell)n_2)/n) \rangle, \\ & \langle \cos(2\pi(-(k + \ell)n_1 + kn_2)/n) \rangle, \langle \sin(2\pi(-(k + \ell)n_1 + kn_2)/n) \rangle, \\ & \langle \cos(2\pi(kn_1 - (k + \ell)n_2)/n) \rangle, \langle \sin(2\pi(kn_1 - (k + \ell)n_2)/n) \rangle, \\ & \langle \cos(2\pi(\ell n_1 + kn_2)/n) \rangle, \langle \sin(2\pi(\ell n_1 + kn_2)/n) \rangle, \\ & \left. \langle \cos(2\pi(-(k + \ell)n_1 + \ell n_2)/n) \rangle, \langle \sin(2\pi(-(k + \ell)n_1 + \ell n_2)/n) \rangle \right] \end{aligned}$$

with the correspondence

m	36(II)	81(IV)	81(V)	81(VI)	108(IV)	108(V)	108(VI)
(k, ℓ)	(6, 3)	(4, 2)	(6, 2)	(6, 4)	(4, 1)	(5, 2)	(7, 1)
m	324(IV)–324(XV)						
(k, ℓ)	(2, 1), (3, 1), (3, 2), (4, 3), (5, 1), (5, 3), (5, 4), (6, 1), (6, 5), (7, 2), (7, 3), (8, 1)						

For example, the basis vector $\mathbf{q}_1^{(3)}$ represents a hexagon with $D = 3$ (Fig. A1(a)); the basis vectors $\mathbf{q}_i^{(4)}$ ($i = 1, 2, 3$) and $\mathbf{q}_i^{(81(\text{I}))}$ ($i = 1, \dots, 6$) express stripe patterns (Figs. A1(b)–(c)). Figure A2 depicts patterns with hexagonal symmetry that are not presented in Fig. 5.

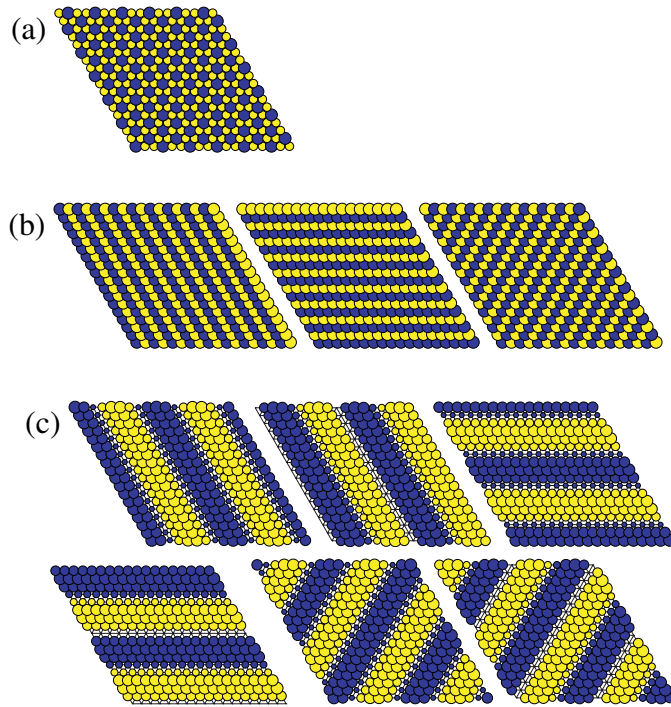


Figure A1: Spatial patterns expressed by basis vectors. (a) $q_1^{(3)}$. (b) $q_i^{(4)}$ ($i = 1, 2, 3$). (c) $q_i^{(81(1))}$ ($i = 1, \dots, 6$). A blue circle denotes a positive component, a yellow circle indicates a negative one, and the area of a circle expresses the magnitude of the component.

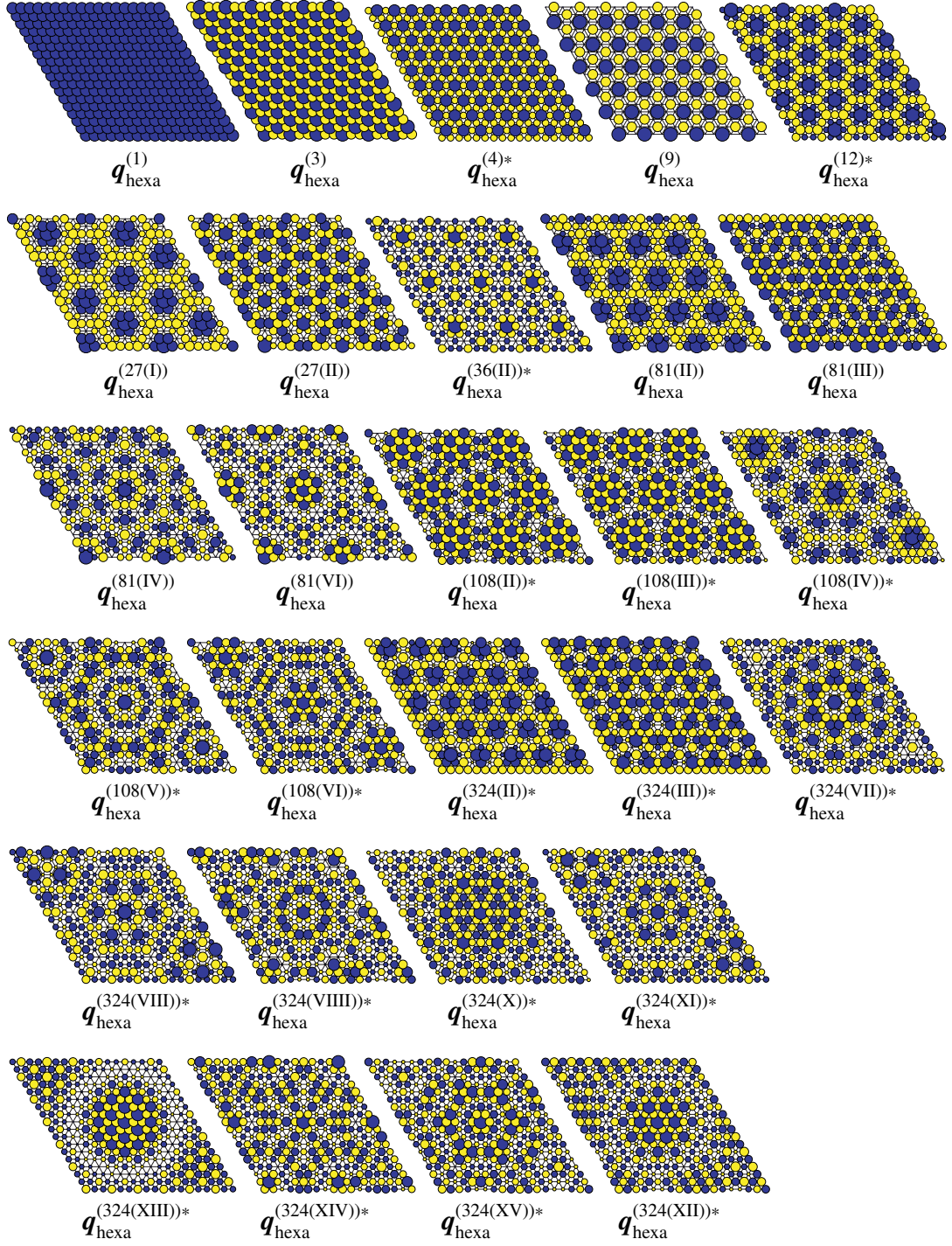


Figure A2: Patterns with hexagonal symmetry other than those given in Fig. 1. Hexagons centered at $(n_1, n_2) = (9, 9)$ are expressed by $q_{\text{hexa}}^{(m)*}$; a blue circle denotes a positive component, a yellow circle indicates a negative one, and the area of a circle expresses the magnitude of the component.

B. Spectrum analysis of Eastern USA

Based on population size, cities in Eastern USA were classified from an A-center at New York, B-centers at Chicago, Dallas, Houston, Washington, and Atlanta, . . . to F-centers as listed in Table B1. The results of the spectrum analysis that are not introduced in Section 5 are presented in Figs. B1–B4. The largest spectrum (except for that of the uniform state for $m = 1$) is associated with the core–satellite pattern $q^{\text{Core–satellite}}$, except for Middle Atlantic Domain I, for which $q^3 \text{ hexagons}$ is predominant. The results for the four domains in Gulf Coast Region (Fig. B1) were used to arrive at the clearest hexagonal distribution of cities (Fig. 13(b)). Those for the five domains in South Atlantic Region (Fig. B2) were assembled to arrive at the fine hexagonal distribution (Fig. 15). Those in East North Central Region (Fig. B3) were used to arrive at the T-shaped distribution in Fig. 15. Middle Atlantic Domain I has a long narrow network from Boston to Washington via New York City (Fig. B4).

Table B1: City population size classification in Eastern USA (2014/07/01). (Metropolitan and micropolitan statistical areas are geographic entities delineated by the Office of Management and Budget (OMB) for use by federal statistical agencies in collecting, tabulating, and publishing federal statistics.)

Name of center	Name of city	Population
A-center ($\lambda \geq 10,000,000$)	New York City - Newark - Jersey City	20,092,883
B-center ($5,000,000 \leq \lambda < 10,000,000$)	Chicago - Naperville - Elgin	9,554,598
	Dallas - Fort Worth - Arlington	6,954,330
	Houston - The Woodlands - Sugar Land	6,490,180
	Washington - Arlington - Alexandria	6,033,737
	Atlanta - Sandy Springs - Roswell	5,614,323
C-center ($3,500,000 \leq \lambda < 5,000,000$)	Boston - Cambridge - Newton	4,732,161
	Detroit - Warren - Dearborn	4,296,611
D-center ($2,000,000 \leq \lambda < 3,500,000$)	St. Louis	2,806,207
	Charlotte - Concord - Gastonia	2,380,314
	Pittsburgh	2,355,968
	San Antonio - New Braunfels	2,328,652
	Cincinnati	2,149,449
	Kansas City	2,071,133
	Cleveland - Elyria	2,063,598
E-center ($1,000,000 \leq \lambda < 2,000,000$)	Columbus (OH)	1,994,536
	Indianapolis - Carmel - Anderson	1,971,274
	Nashville - Davidson - Murfreesboro - Franklin	1,792,649
	Virginia Beach - Norfolk - Newport News	1,716,624
	Milwaukee - Waukesha - West Allis	1,572,245
	Jacksonville	1,419,127
	Memphis	1,343,230
	Oklahoma City	1,336,767
	Louisville/Jefferson County	1,269,702
	Richmond	1,260,029
	New Orleans - Metairie	1,251,849
	Raleigh	1,242,974
	Birmingham - Hoover	1,143,772
	Grand Rapids - Wyoming	1,027,703

Table B1 (continued)

Name of center	Name of city	Population
F-center	Tulsa	969,224
(100,000 ≤ λ < 1,000,000)	Omaha - Council Bluffs	904,421
	Greenville - Anderson - Mauldin	862,463
	Knoxville	857,585
	Columbia (SC)	800,495
	Greensboro - High Point	746,593
	Little Rock - North Little Rock - Conway	729,135
	Charleston - North Charleston	727,689
	Wichita	641,076
	Des Moines - West Des Moines	611,549
	Toledo	607,456
	Augusta - Richmond County	583,632
	Jackson	577,564
	Chattanooga	544,559
	Lexington - Fayette	494,189
	Pensacola - Ferry Pass - Brent	474,081
	Springfield	452,297
	Shreveport - Bossier City	445,142
	Huntsville	441,086
	Myrtle Beach - Conway - North Myrtle Beach	417,668
	Tallahassee	375,751
	Montgomery	373,141
	Savannah	372,708
	Huntington - Ashland	363,325
	Evansville	315,162
	Columbus (GA-AL)	314,005
	Macon	230,450
	Charleston	222,878
	Johnson City	201,091
	Columbia (MO)	172,717
	Terre Haute	171,480
	Albany	154,925
	Dothan	148,095
	Valdosta	143,317
	Anniston - Oxford - Jacksonville	115,916

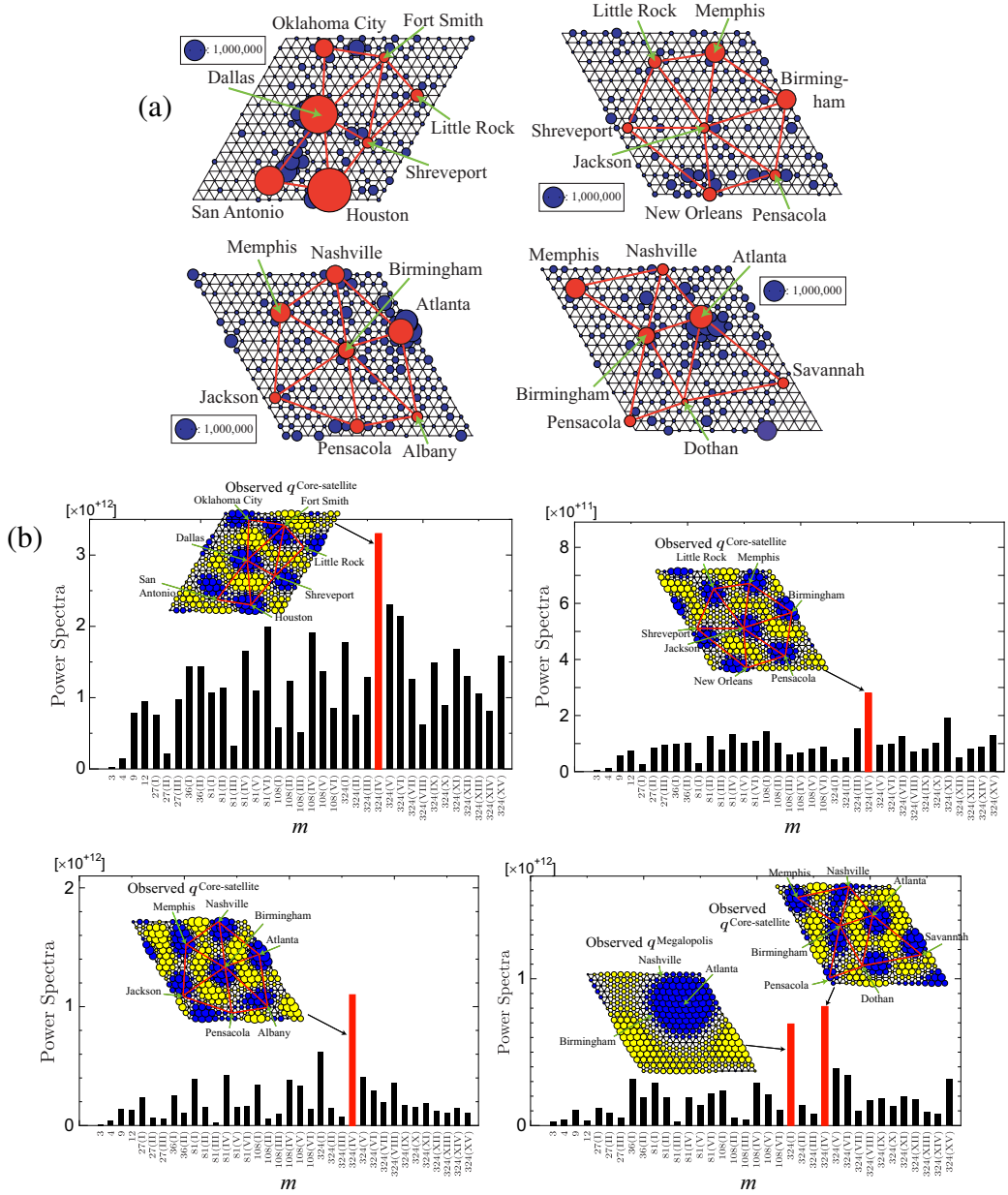


Figure B1: Spectrum analysis for the four domains in Gulf Coast Region. (a) Discretized population map and distributions of cities. The area of a circle denotes the population size and a series of red lines denotes the distribution of cities. (b) Power spectra and the spatial patterns of the predominant spectrum $q^{\text{Core-satellite}}$. A blue circle denotes a positive component, a yellow circle indicates a negative one, and the area of a circle expresses the magnitude of the component.

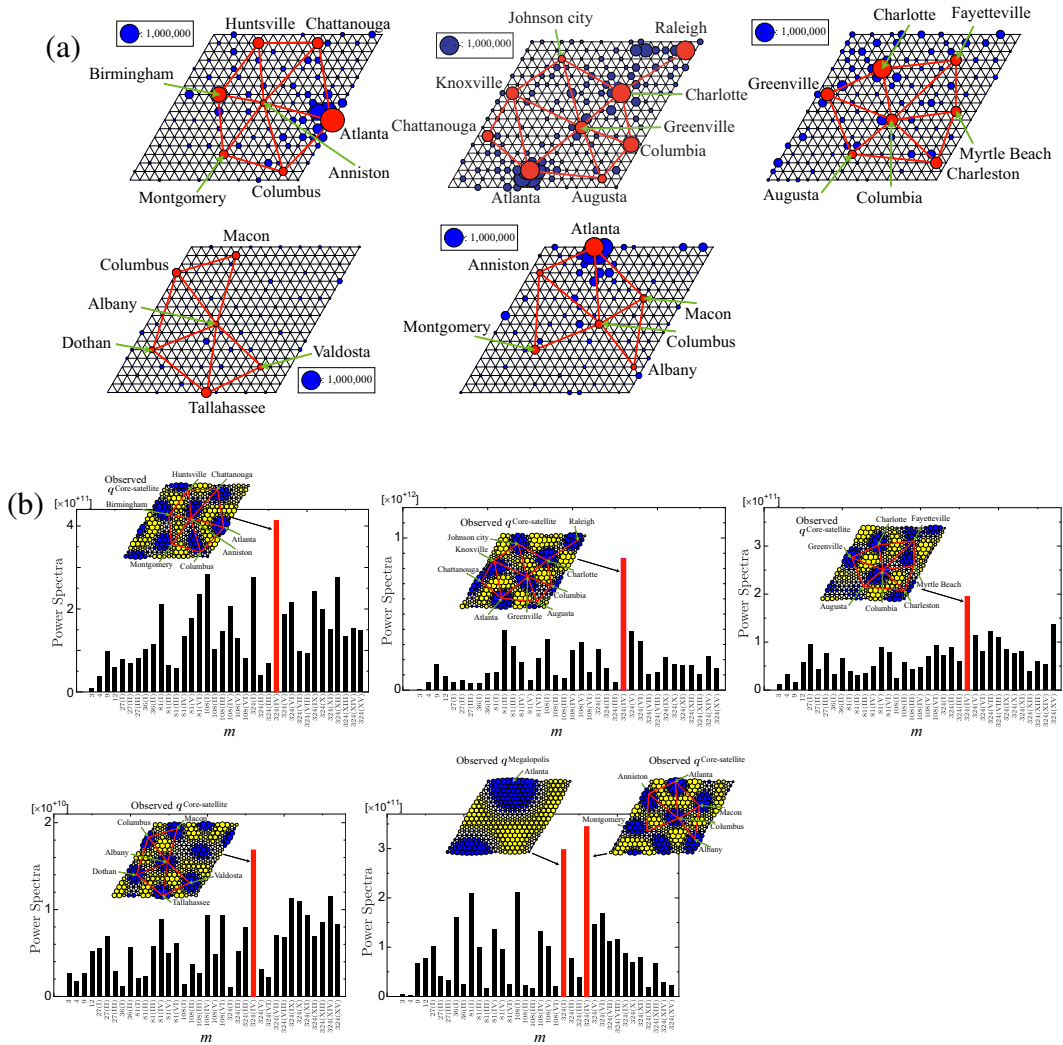


Figure B2: Spectrum analysis for the five domains in South Atlantic Region. (a) Discretized population map and distributions of cities. The area of a circle denotes the population size and a series of red lines denotes the distribution of cities. (b) Power spectra and the spatial patterns of the predominant spectrum $q^{\text{Core-satellite}}$. A blue circle denotes a positive component, a yellow circle indicates a negative one, and the area of a circle expresses the magnitude of the component.

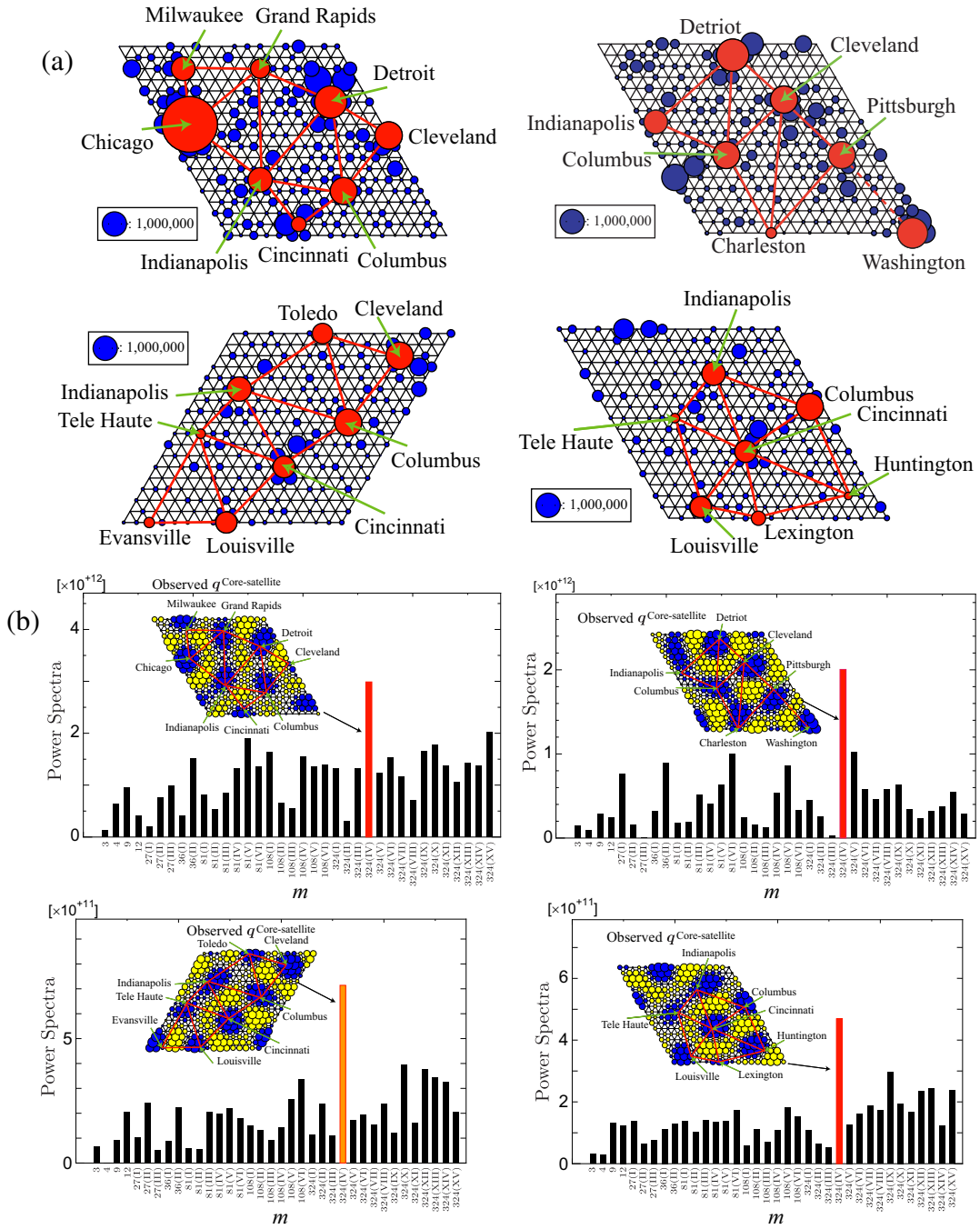


Figure B3: Spectrum analysis for the four domains in East North Central Region. (a) Discretized population map and distributions of cities. The area of a circle denotes the population size and a series of red lines denotes the distribution of cities. (b) Power spectra and the spatial patterns of the predominant spectrum $q^{\text{Core-satellite}}$. A blue circle denotes a positive component, a yellow circle indicates a negative one, and the area of a circle expresses the magnitude of the component.

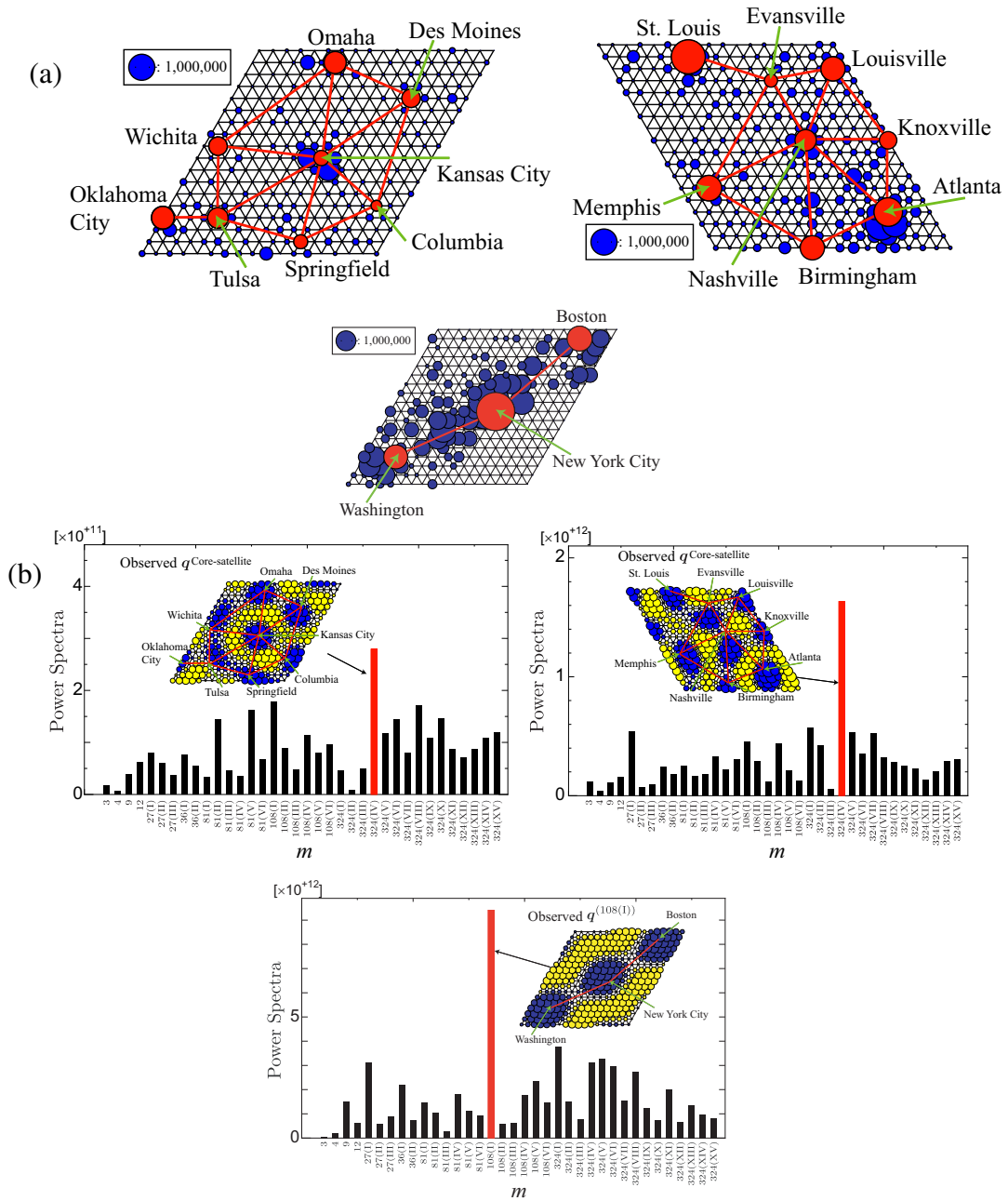


Figure B4: Spectrum analysis for West North Central Domains II and III and Middle Atlantic Domain I. (a) Discretized population map and distributions of cities. The area of a circle denotes the population size and a series of red lines denotes the distribution of cities. (b) Power spectra and spatial patterns of predominant spectra. A blue circle denotes a positive component, a yellow circle indicates a negative one, and the area of a circle expresses the magnitude of the component.